

# CKI $\epsilon$ / $\delta$ -dependent phosphorylation is a temperature-insensitive, period-determining process in the mammalian circadian clock

Yasushi Isojima<sup>a,b,1</sup>, Masato Nakajima<sup>c,1</sup>, Hideki Ukai<sup>c,1</sup>, Hiroshi Fujishima<sup>c</sup>, Rikuhiko G. Yamada<sup>a</sup>, Koh-hei Masumoto<sup>c</sup>, Reiko Kiuchi<sup>a,b</sup>, Mayumi Ishida<sup>c</sup>, Maki Ukai-Tadenuma<sup>c</sup>, Yoichi Minami<sup>c</sup>, Ryotaku Kito<sup>c</sup>, Kazuki Nakao<sup>d</sup>, Wataru Kishimoto<sup>c</sup>, Seung-Hee Yoo<sup>e,f,g</sup>, Kazuhiro Shimomura<sup>f,h</sup>, Toshifumi Takao<sup>i</sup>, Atsuko Takano<sup>j</sup>, Toshio Kojima<sup>a</sup>, Katsuya Nagai<sup>j</sup>, Yoshiyuki Sakaki<sup>a</sup>, Joseph S. Takahashi<sup>e,f,g,h,2</sup>, and Hiroki R. Ueda<sup>c,k,l,2</sup>

<sup>a</sup>Comparative Systems Biology Team, Genomic Science Center and <sup>b</sup>Developmental Systems Modeling Team, Advanced Computational Sciences Department, RIKEN, 1-7-22, Suehiro-cho, Tsurumi, Yokohama 230-0045, Japan; <sup>c</sup>Laboratory for Systems Biology, <sup>k</sup>Functional Genomics Unit, and <sup>d</sup>Animal Resource Unit, RIKEN Center for Developmental Biology, 2-2-3 Minatojima-minamimachi, Chuo-ku, Kobe 650-0047, Japan; <sup>e</sup>Howard Hughes Medical Institute, <sup>f</sup>Department of Neurobiology and Physiology, and <sup>h</sup>Center for Functional Genomics, Northwestern University, 2205 Tech Drive, Evanston, IL 60208; <sup>g</sup>Department of Neuroscience, University of Texas Southwestern Medical Center, Dallas, TX 75390-9111; <sup>i</sup>Laboratory of Protein Profiling and Functional Proteomics, and <sup>j</sup>Laboratory of Proteins Involved in Homeostatic Integration, Institute for Protein Research, Osaka University, Yamadaoka 3-2, Suita, Osaka 565-0871, Japan; and <sup>l</sup>Department of Bioscience, Graduate School of Science, Osaka University, Toyonaka, Osaka 560-0043, Japan

contributed by Joseph S. Takahashi, August 4, 2009 (sent for review June 14, 2009)

**A striking feature of the circadian clock is its flexible yet robust response to various environmental conditions. To analyze the biochemical processes underlying this flexible-yet-robust characteristic, we examined the effects of 1,260 pharmacologically active compounds in mouse and human clock cell lines. Compounds that markedly (>10 s.d.) lengthened the period in both cell lines, also lengthened it in central clock tissues and peripheral clock cells. Most compounds inhibited casein kinase I $\epsilon$  (CKI $\epsilon$ ) or CKI $\delta$  phosphorylation of the PER2 protein. Manipulation of CKI $\epsilon$ / $\delta$ -dependent phosphorylation by these compounds lengthened the period of the mammalian clock from circadian (24 h) to circadian (48 h), revealing its high sensitivity to chemical perturbation. The degradation rate of PER2, which is regulated by CKI $\epsilon$ / $\delta$ -dependent phosphorylation, was temperature-insensitive in living clock cells, yet sensitive to chemical perturbations. This temperature-insensitivity was preserved in the CKI $\epsilon$ / $\delta$ -dependent phosphorylation of a synthetic peptide *in vitro*. Thus, CKI $\epsilon$ / $\delta$ -dependent phosphorylation is likely a temperature-insensitive period-determining process in the mammalian circadian clock.**

chemical biological approach | temperature compensation

The circadian clock is a molecular mechanism underlying endogenous, self-sustained oscillations with a period of  $\approx$ 24 h, manifested in diverse physiological and metabolic processes (1–3). The most striking feature of circadian clock is its flexible yet robust response to various environmental conditions. For example, circadian periodicity varies with light intensity (4–6) while remaining robust over a wide range of temperatures (“temperature compensation”) (1, 3, 7–9). This flexible-yet-robust characteristic is evolutionarily conserved in organisms ranging from photosynthetic bacteria to warm-blooded mammals (3, 10–12), and has interested researchers from a broad range of disciplines. However, despite many genetic and molecular studies (13–22), the detailed biochemical mechanism underlying this characteristic remains poorly elucidated (3).

The simplest explanation for this flexible-yet-robust property is that the key period-determining reactions are insensitive to temperature but responsive to other environmental conditions. Indeed, Pittendrigh proposed the existence of a temperature-insensitive component in the clock system in 1954 (7), and in 1968, he and his colleagues demonstrated that both the wave form and the period of circadian oscillations are invariant with temperature (23). However, the idea of a temperature-insensitive biochemical reaction is counterintuitive, as elementary chemical processes are highly temperature-sensitive. One

exception is the cyanobacterial clock, in which temperature-insensitive enzymatic reactions are observed (24, 25). However, the cyanobacterial clock is quite distinct from other clock systems, and this biochemical mechanism has not been demonstrated in other clocks.

Recently, a chemical-biological approach was proposed to help elucidate the basic processes underlying circadian clocks (26), and high-throughput screening of a large chemical compound library was performed (27). In this report, to analyze systematically the fundamental processes involved in determining the period length of mammalian clocks, we tested 1,260 pharmacologically active compounds for their effect on period length in mouse and human clock cell lines, and found 10 compounds that most markedly lengthened the period of both clock cell lines affected both the central and peripheral circadian clocks. Most compounds inhibited CKI $\epsilon$  or CKI $\delta$  activity, suggesting that CKI $\epsilon$ / $\delta$ -dependent phosphorylation is an important period-determining process in the mammalian circadian clock. Surprisingly, the degradation rate of endogenous PER2, which is regulated by CKI $\epsilon$ -dependent phosphorylation (28) and probably by CKI $\delta$ -dependent phosphorylation, was temperature-insensitive in the living clock cells, and the temperature-insensitivity was preserved even for the *in vitro* CKI $\epsilon$ / $\delta$ -dependent phosphorylation of a synthetic peptide derived from PER2. These results suggest that this period-determining process is flexible in response to chemical perturbation yet robust in the face of temperature perturbations. Based on these findings, we propose that CKI $\epsilon$ / $\delta$ -dependent phosphorylation is a temperature-insensitive period-determining process in the mammalian circadian clock.

## Results

**Ten Compounds Markedly Lengthened Period Length.** We examined 1,260 pharmacologically active chemical compounds from the

Author contributions: Y.I., M.N., H.U., T.T., K. Nagai, and H.R.U. designed research; Y.I., M.N., H.U., H.F., K.-h.M., R. Kiuchi, M.I., M.U.-T., Y.M., R. Kito, K. Nakao, W.K., S.-H.Y., K.S., A.T., T.K., Y.S., and J.S.T. performed research; W.K. contributed new analytic tools; R.G.Y. analyzed data; and Y.I., M.N., H.U., and H.R.U. wrote the paper.

The authors declare no conflict of interest.

Freely available online through the PNAS open access option.

<sup>1</sup>Y.I., M.N., and H.U. contributed equally to this work.

<sup>2</sup>To whom correspondence may be addressed. E-mail: uedah-tky@umin.ac.jp or j-takahashi@northwestern.edu.

This article contains supporting information online at [www.pnas.org/cgi/content/full/0908733106/DCSupplemental](http://www.pnas.org/cgi/content/full/0908733106/DCSupplemental).

LOPAC<sup>1280</sup> library for their effect on circadian period length in mammalian clock cell lines, NIH 3T3-*mPer2-Luc* and U2OS-*hPer2-Luc* (Table S1 and Table S2 and *SI Text*). We identified 10, all with period-lengthening effects, that substantially altered the period in both cell lines ( $> +10$  s.d. or  $< -10$  s.d.,  $\approx 2.0$ – $3.0$  h) (Fig. S1 A and D and Tables S3 and S4). These compounds, labeled “potent,” also lengthened the period of primary cultures of mouse embryonic fibroblasts (MEFs, as peripheral clock cells) (Fig. S1 B and E) and slice cultures of suprachiasmatic nucleus (SCN; as central clock tissue) (Fig. S1 C and E). These results supported the idea that the potent compounds alter canonical clock processes.

**Potent Compounds Inhibit CKI $\epsilon/\delta$  Enzymatic Activity.** Most of the proposed targets of the 10 potent compounds on the list in Table S3 have not been identified as components of the mammalian circadian clock, although one of the 10 is an inhibitor of CK2, recently found as a component of the mammalian circadian clock (29, 30). The potent protein kinase inhibitors SB202190, SP600125, and roscovitine were previously reported to inhibit CKI in addition to their primary targets (31, 32). Since even specific protein kinase inhibitors also usually affect other kinases (31, 33), we hypothesized that the seven protein kinase inhibitors that we identified suppress CKI activity in addition to their primary targets.

To examine this hypothesis, we performed the siRNA knockdown of CKI genes, as well as the genes related to the 10 potent compounds (Fig. 1 A–C and Fig. S2 B–G). The knockdown of *CKI $\epsilon$*  or *CKI $\delta$*  exhibited the greatest period-lengthening effects (Fig. 1B), more than 28 h in CT, whereas knockdown of other genes showed no or only a slight effect (Fig. S2 B–G). Moreover, the combinatorial knockdown of *CKI $\epsilon$*  and *CKI $\delta$*  additively lengthened the period of circadian oscillations to over 30 h in CT (Fig. 1C), supporting the idea that *CKI $\epsilon/\delta$*  play one of the most important roles in the period-determination processes of mammalian circadian clocks. These results suggest that at least some of our compounds were not acting via their primary target, but through inhibition of *CKI $\epsilon/\delta$* .

The inhibitory effect of the potent compounds on *CKI $\epsilon/\delta$*  activity was confirmed by the in vitro *CKI $\epsilon$*  or *CKI $\delta$*  kinase assay. Importantly, nine of the 10 compounds [i.e., not 17 $\alpha$ -hydroxyprogesterone (17-OHP)] strongly inhibited the catalytic domain of wild-type *CKI $\epsilon$* , lacking the C-terminal regulatory domain ( $\Delta$ *CKI $\epsilon$* ) as effectively as or better than IC261, a specific inhibitor of CKI (Fig. 1D). SP600125 and TG003, which dramatically extended the circadian period and potently inhibited  $\Delta$ *CKI $\epsilon$*  activity, strongly inhibited both activity of the  $\Delta$ *CKI $\epsilon$*  and catalytic domain of *CKI $\delta$*  ( $\Delta$ *CKI $\delta$* ), with lower  $IC_{50}$  ( $< 0.55$   $\mu$ M) than the  $IC_{50}$  of IC261 (about 4  $\mu$ M), whereas 17-OHP did not inhibit both of  $\Delta$ *CKI $\epsilon$*  and  $\Delta$ *CKI $\delta$*  (Fig. 1E). Since double knockdown of the *CKI $\epsilon$*  and *CKI $\delta$*  genes using siRNA had additive effects on period lengthening (Fig. 1C), and these chemical compounds, except 17-OHP, inhibited *CKI $\epsilon$*  and *CKI $\delta$*  similarly, they probably acted on both CKIs to affect the period length of circadian oscillations.

We also examined the effect of potent compounds on the stability of the mPER2 protein, which was regulated by *CKI $\epsilon$*  (28) (and probably by *CKI $\delta$* ) in non-clock cell, 293T cells. Fig. S3 A and B show that the two putative CKI inhibitors significantly enhanced the stability and slowed the degradation rate of LUC::mPER2 ( $P < 0.01$ , one-way ANOVA), whereas 17-OHP did not significantly affect LUC::mPER2 stability ( $P = 0.18$ , one-way ANOVA). These results were supported by immunoblot experiments (Fig. S4). This degradation rate of overexpressed LUC::mPER2 was not affected without the co-overexpression of *CKI $\epsilon$*  (*tau*) (Fig. S3C;  $P = 0.193$  for SP600125 and  $P = 0.728$  for TG003; two-way ANOVA), presumably because relative expression levels of LUC::mPER2 in 293T cells compared with *CKI $\epsilon/\delta$*

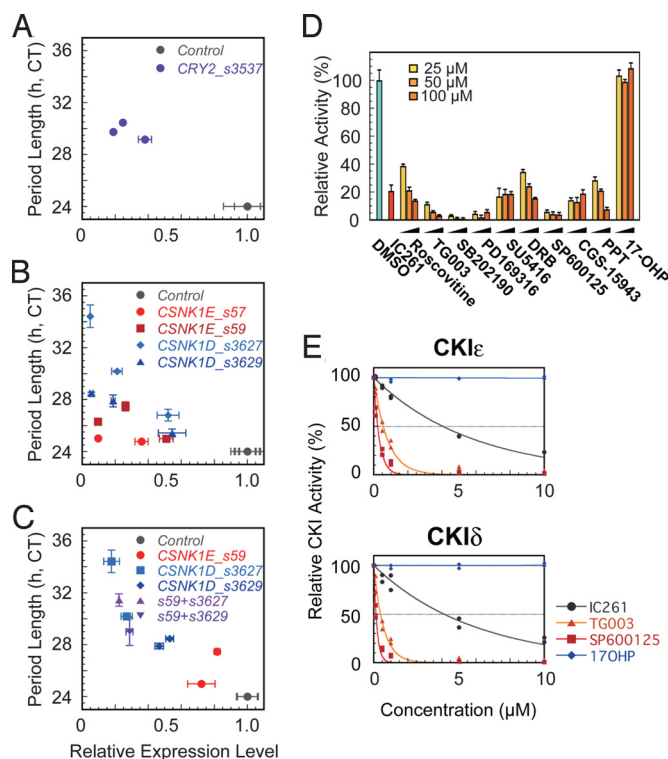


**Fig. 1.** Effects of knockdowns of *CSNK1s* on the period length and effect of potent compounds on the *CKI $\epsilon/\delta$*  activity in vitro. (A–C) Graphs indicate relationship between gene knockdown effects and period length in U2OS-*hPer2-Luc* cells. The x-axis indicates the expression level of genes relative to the samples transfected with control siRNA. The y-axis indicates the period length, described in circadian time (CT), with the control samples assigned as 24 h. Each symbol represents the mean  $\pm$  SEM of independent experiments ( $n \geq 3$ ). (A) The effect of *CRY2* knockdown as a positive control. (B) Gene knockdowns of *CKI $\epsilon/\delta$* . *CSNK1E*, *CKI $\epsilon$* ; *CSNK1D*, *CKI $\delta$* . (C) Effect of the double knockdown of *CSNK1E* and *CSNK1D*. The gene expression level represents the total amount of *CKI $\delta$*  and *CKI $\epsilon$* . (D)  $\Delta$ *CKI $\epsilon$*  phosphorylation activity for a synthetic mPER2 peptide in the presence of chemical compounds [25, 50, or 100  $\mu$ M for the 10 compounds, 100  $\mu$ M for IC261] was measured using a modified IMAP assay with 100  $\mu$ M ATP. The average results for each condition are shown as the relative activity compared to the control condition (DMSO). Error bars denote 1 s.d. (E) Dose-dependent effects of SP600125 and TG003 on  $\Delta$ *CKI $\epsilon/\delta$*  phosphorylation activity.  $\Delta$ *CKI $\epsilon/\delta$*  phosphorylation activity was measured in the presence of compounds at the indicated concentrations. Each symbol indicates the activity relative to the control condition in two independent experiments. The lines are approximate functions using the equation:  $y = 100e^{-ax}$ . The  $IC_{50}$ s for *CKI $\epsilon$*  calculated from the equations were 4.0, 0.55, and 0.22  $\mu$ M for IC261, TG003, and SP600125, respectively, and for *CKI $\delta$*  were 4.1, 0.40, and 0.13  $\mu$ M.

were much higher than in MEFs. We used *CKI $\epsilon$* (*tau*) for these assays because the degradation rate with co-overexpression of *CKI $\epsilon$* (*tau*) was faster than that of *CKI $\epsilon$* (wt), which enable us to measure the PER2 degradation rate precisely. We next confirmed that the stability of LUC-fused mPER1 protein (LUC::mPER1), the closest relative of mPER2, was also decreased with co-expression of *CKI $\epsilon$* (*tau*) as well as LUC::mPER2, whereas LUC-fused mBMAL1 (LUC::mBMAL1) and native LUC were not (Fig. S5). These results suggest that the inhibitory effect of the potent compounds on *CKI $\epsilon/\delta$*  activity is the primary mechanism by which they lengthened the period of clock cells. In contrast, 17-OHP apparently functions via a different mechanism.

**Flexibility and Robustness of a Period Determination Process.** To explore how important this process is for determining the period

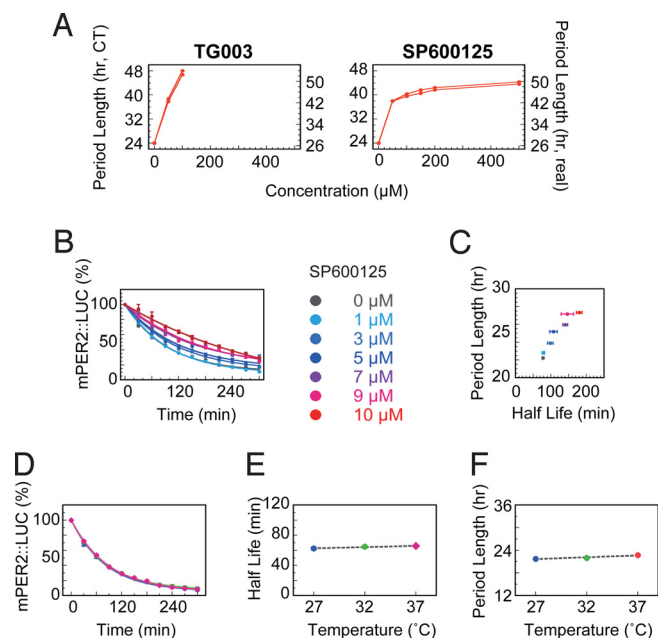


**Fig. 2.** Flexibility and robustness of a period-determination process of the mammalian circadian clock. (A) Dose-dependent effects of SP600125 and TG003 on period length in U2OS-*hPer2-Luc* cells. The period length is indicated both in real-time (right axis) and in circadian time (left axis). For circadian time, the average period length in two independent control experiments was assigned as 24.0 h. The two lines in each graph correspond to two independent experiments. Each value represents the mean  $\pm$  SEM. At the concentrations without data points, the cells behaved arrhythmically. (B and C) Dose-dependent effect of SP600125 on the period length and degradation rate of mPER2::LUC in *mPer2<sup>Luc</sup>* MEFs. A pair of plates with cultured *mPer2<sup>Luc</sup>* MEFs, to which 0 to 10  $\mu\text{M}$  SP600125 was applied, were prepared. One was used to measure mPER2::LUC decay and the other to determine the period. (B) Decay of mPER2::LUC bioluminescence in *mPer2<sup>Luc</sup>* MEFs. The degradation of mPER2::LUC protein was monitored after the administration of CHX to MEFs. The time-course data of each sample were normalized to approximate functions in which time point 0 was 100%. Each value represents the mean  $\pm$  SEM. The lines represent approximated curves in which  $y = 100$  at time = 0 and  $y = 50$  at the averaged half-life time. The colors in order from gray to blue to red represent the concentration of SP600125 with 0.25% DMSO ( $n = 6$ ). (C) Correlation between the period length and degradation rate of mPER2::LUC in *mPer2<sup>Luc</sup>* MEFs with the administration of SP600125. Each value represents the mean  $\pm$  SEM ( $n = 6$ ). (D) Temperature dependency of decay of the mPER2::LUC bioluminescence in *mPer2<sup>Luc</sup>* MEFs. The degradation of mPER2::LUC protein was monitored after the addition of CHX to MEFs. The time-course data of each sample were normalized to an approximate function in which time point 0 was 100%. Each value represents the mean  $\pm$  SEM of the normalized data. The lines represent an approximated curve in which  $y = 100$  at time = 0 and  $y = 50$  at the averaged half-life time. The blue dots and line indicate the data at 27  $^{\circ}\text{C}$ ; green, 32  $^{\circ}\text{C}$ ; and magenta, 37  $^{\circ}\text{C}$  ( $n = 23$ ). (E) Temperature compensation in the half-lives of the mPER2::LUC protein. The graph indicates the mean  $\pm$  SEM. The gray broken line indicates the approximated line described by the equation:  $y = 53.69 + 0.333x$ , and the  $Q_{10}$  value between 27 and 37  $^{\circ}\text{C}$  calculated from the equation is 0.950. (F) Temperature compensation in the period length of *mPer2<sup>Luc</sup>* MEFs. The graph indicates the mean  $\pm$  SEM. The gray broken line indicates the approximated line described by the equation:  $y = 19.02 + 0.097x$ , and the  $Q_{10}$  value between 27 and 37  $^{\circ}\text{C}$  calculated from the equation is 0.957.

length of the mammalian circadian clock, we examined the effects of these two compounds on the circadian period length at higher concentrations (50–500  $\mu\text{M}$ ). Interestingly, the higher concentrations approximately doubled the period length (to 53.98 and 52.50 h at 100  $\mu\text{M}$  for TG003, and 48.63 and 49.74 h at 500  $\mu\text{M}$  for SP600125) relative to the control U2OS-*hPer2-Luc* cells (26.89 and 27.02 h) (Fig. 2A). Therefore, these results suggest that a period-determining process mediated by CKI $\epsilon/\delta$ -

dependent phosphorylation is remarkably flexible to chemical perturbation, since a single compound lengthened the period from circadian ( $\approx 24$  h) to almost circadian ( $\approx 48$  h).

To further confirm this flexibility, we next investigated the sensitivity of this process to chemical perturbation in living clock cells by using *mPer2<sup>Luc</sup>* MEFs. We observed that the period length of the circadian oscillation in MEFs correlated well with the mPER2::LUC stability under the administration of a potent compound (Fig. 2B and C). Given this strong correlation, we concluded that CKI $\epsilon/\delta$  activity on the PER2 protein is one of the most important period-determining processes in the mammalian circadian oscillator.

If important period-determination processes were highly sensitive to temperature, it would be very difficult to maintain the temperature compensation over the entire circadian period. Thus, we next investigated the temperature dependency of this process in living clock cells by using *mPer2<sup>Luc</sup>* MEFs. We found that the degradation rate of mPER2::LUC and the period length were completely temperature-insensitive in the MEFs (Fig. 2D–F). The observed temperature-insensitivity seemed to reflect a molecular property of the endogenous mPER2 protein, because the degradation rate of LUC is sensitive to temperature in mammalian cells (Fig. 4A and B). These results imply that the period-determination process, which was sensitive to chemical perturbation, was remarkably robust against physical perturbation such as temperature differences.

**CKI $\epsilon/\delta$  Activity Is Insensitive to Temperature.** To examine the biochemical foundation underlying the observed temperature-insensitivity, we analyzed the phosphorylation activity of CKI $\epsilon$  and CKI $\delta$  in vitro. To facilitate this analysis, we designed a synthetic peptide substrate derived from the putative  $\beta\text{TrCP}$ -binding region of mouse PER2 (referred to here as  $\beta\text{TrCP}$ -peptide) (Fig. S6A), because this region is important for phosphorylation-dependent degradation of PER2 in the mammalian clock system (34). We first used just the catalytic domain of wild-type CKI $\epsilon$ , lacking the C-terminal regulatory domain [ $\Delta\text{CKI}\epsilon(\text{wt})$ ] to prevent potential confusion that could result from the autophosphorylation of this regulatory domain and the subsequent repression of CKI $\epsilon$  kinase activity. This use of the catalytic domain was also justified by evidence that CKI $\epsilon$  is kept in a dephosphorylated, active state in vivo (35).

Under this experimental setup, we successfully recapitulated, at least partially, the enhanced phosphorylation seen with a  $\Delta\text{CKI}\epsilon$  *tau* mutation [ $\Delta\text{CKI}\epsilon(\text{tau})$ ] (36) in comparison with  $\Delta\text{CKI}\epsilon(\text{wt})$  at 35  $^{\circ}\text{C}$  (Fig. 3A, red). Consistent with our other findings,  $\Delta\text{CKI}\epsilon(\text{wt})$  and  $\Delta\text{CKI}\epsilon(\text{tau})$  phosphorylated the peptide substrate at similar rates whether at 25  $^{\circ}\text{C}$  (Fig. 3A, blue) or 35  $^{\circ}\text{C}$ , indicating a strong temperature-insensitivity ( $Q_{10} = 1.0$ ) [Fig. 3D,  $\Delta\text{CKI}\epsilon(\text{wt})$  and  $\Delta\text{CKI}\epsilon(\text{tau})$ ]. Similar temperature-insensitivity were also observed by using catalytic domain of wild-type CKI $\delta$  lacking the C-terminal regulatory domain [ $\Delta\text{CKI}\delta(\text{wt})$ ] ( $Q_{10} = 1.2$ ) [Fig. 3D,  $\Delta\text{CKI}\delta$ ].

The temperature-insensitivity of the CKI $\epsilon$  reaction depended substantially on the phosphorylation state of CKI $\epsilon$  itself, because the  $Q_{10}$  of the autophosphorylated full-length construct (preincubated with ATP) was greater than for the isolated catalytic domain (Fig. 3B and D, CKI $\epsilon$ , preincubated). We also confirmed an earlier report that preincubating full-length CKI $\epsilon$  with ATP repressed its enzymatic activity ( $\approx 15$ -fold and 8-fold at 25  $^{\circ}$  and 35  $^{\circ}\text{C}$ , respectively) (37); this was probably due to the autophosphorylation of the C-terminal regulatory domain (Fig. S6B and C). The effects of autophosphorylation on enzymatic activity were also recapitulated by a mutant in which the eight autophosphorylated serine residues in the C-terminal regulatory domain (37) were replaced with glutamate [Fig. 3D, CKI $\epsilon$ (D8)]. Using this autophosphorylation mutant, we observed both a slightly enhanced temperature sensitivity [ $Q_{10} = 1.3$ , an increase

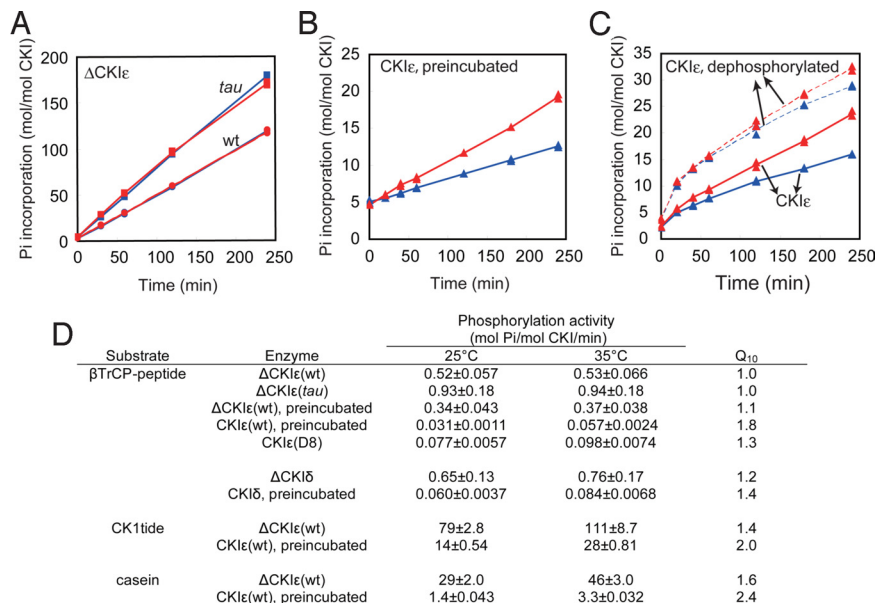


**Fig. 3.** Temperature insensitivity of the CKI $\epsilon/\delta$  phosphorylation activity. (A) Temperature dependency of the  $\Delta$ CKI $\epsilon$ (wt) (circles) and  $\Delta$ CKI $\epsilon$  (*tau*) (squares) phosphorylation activity for the  $\beta$ TrCP-peptide substrate. Assays were performed at 25 °C (blue) and 35 °C (red). (B) Phosphorylation activity of full-length CKI $\epsilon$ (wt) autophosphorylated by preincubation with ATP. Assays were performed at 25 °C (blue) and 35 °C (red). (C) Temperature dependency of the full-length CKI $\epsilon$  phosphorylation activity for the  $\beta$ TrCP-peptide substrate. Phosphorylation activity of full-length CKI $\epsilon$ (wt) (CKI $\epsilon$ , solid line), and CKI $\epsilon$ (wt) dephosphorylated with  $\lambda$  protein phosphatase (CKI $\epsilon$ , dephosphorylated) (broken line). Assays were performed at 25 °C (blue) and 35 °C (red). (D) Summary for temperature dependency of CKI $\epsilon/\delta$  enzymatic activities.

of 0.3 compared with  $\Delta$ CKI $\epsilon$ (wt)] and a repression of enzymatic activity ( $\approx$ 6-fold and  $\approx$ 5-fold at 25 °C and 35 °C, respectively). We confirmed these effects on the time-course of phosphorylation by full-length CKI $\epsilon$  that was not preincubated with ATP: As the incubation time increased (and probably as autophosphorylation increased), the enzymatic activity slowed (slopes of the curves decreased), and the temperature sensitivity (i.e., the difference in slope between 25 °C and 35 °C) increased (Fig. 3C, CKI $\epsilon$ ). We further confirmed these effects on the time course of phosphorylation using dephosphorylated full-length CKI $\epsilon$  without preincubation (Fig. S6B and C) and found that the enzymatic activity slowed substantially and the temperature sensitivity increased between the first hour and the next 3 h (Fig. 3C, CKI $\epsilon$ , dephosphorylated). The effect of autophosphorylation on the temperature dependency was more prominent with CKI $\epsilon$  than with the closely related CKI $\delta$ ; the repression of enzymatic activity was, however, also observed for CKI $\delta$  (Fig. 3D,  $\Delta$ CKI $\delta$  and CKI $\delta$ , preincubation).

PER2 phosphorylation is a complicated process involving multiple phosphorylation sites (38). To explore the temperature dependency of CKI $\epsilon$  with another substrate, we designed a synthetic peptide substrate derived from the region near the functional amino acids in PER2, which is responsible for familial advanced sleep phase syndrome (FASPS) (referred to here as FASPS-peptide) (Fig. S6A). We chose this site because a serine at position 662 of human PER2 (amino acid 659 of mPER2) was identified as a mutation for FASPS (39). We found that the phosphorylation of FASPS-peptide by  $\Delta$ CKI $\epsilon$ (wt) was also temperature-insensitive, with a  $Q_{10} = 1.2$ , whereas the phosphorylation by  $\Delta$ CKI $\epsilon$ (*tau*) was more temperature-sensitive ( $Q_{10} = 1.6$ ) (Fig. S6D). These results with the FASPS- and  $\beta$ TrCP-peptides suggest that CKI-dependent phosphorylation can be temperature-insensitive, depending on both the substrate and the state of the enzyme.

Since CKI $\epsilon/\delta$  is involved in a variety of other biological processes, we next investigated the temperature dependency of its activity for two clock-unrelated substrates: casein, a conven-

tional protein substrate, and CK1tide, a commercially available peptide substrate for CKI $\epsilon/\delta$ , which was a peptide substrate phosphorylated at two residues N-terminal of CKI $\epsilon/\delta$  phosphorylation site. Enhanced temperature sensitivity was observed for these substrates ( $Q_{10} = 1.6$  for casein and 1.4 for CK1tide) (Fig. 3D), although it was still less than expected for canonical enzymatic reactions ( $Q_{10} = 2-3$ ). As with  $\beta$ TrCP-peptide, enhanced temperature sensitivity due to autophosphorylation was also observed for these substrates ( $Q_{10} = 2.4$  for casein, an increase of 0.8; and  $Q_{10} = 2.0$  for CK1tide, an increase of 0.6) (Fig. 3D), confirming that the temperature insensitivity depends substantially on the substrate as well as on the state of the enzyme (see also *SI Text*).

Although we demonstrated that the enzymatic activity of CKI $\epsilon$  was temperature-insensitive for two synthetic peptide substrates ( $\beta$ TrCP-peptide and FASPS-peptide) derived from mPER2 as described above, it was still unclear if this temperature insensitivity would hold for the full-length mPER2 protein, which may have multiple phosphorylation sites outside the putative  $\beta$ TrCP-binding region and FASPS site. We therefore examined the degradation rate of mPER2::LUC, which was overexpressed in mouse clock cells (NIH 3T3) and compared it to that of LUC. As expected, the degradation rate of LUC was highly sensitive to temperature between 27 °C and 32 °C ( $Q_5 = 2.08$  and 2.10, extrapolated  $Q_{10} = 4.33$  and 4.41, without or with  $\Delta$ CKI $\epsilon$ , respectively; Fig. 4A, B, and E). The  $Q_5$  represent the relative change of a physical property as a consequence of increasing the temperature by 5 °C. On the other hand, the degradation rate of mPER2::LUC was less sensitive to temperature ( $Q_5 = 1.51$ , extrapolated  $Q_{10} = 2.28$ ; Fig. 4C and E). Importantly, enhancing the enzymatic reaction between mPER2 and CKI $\epsilon$  by additionally expressing the catalytic domain of CKI $\epsilon$  ( $\Delta$ CKI $\epsilon$ ) in NIH 3T3 cells recapitulated the temperature insensitivity of the mPER2::LUC degradation rate ( $Q_5 = 1.22$ , extrapolated  $Q_{10} = 1.49$ ; Fig. 4D and E). Based on these results together with our finding in *mPer2<sup>Luc</sup>* MEFs (Fig. 2D-F), we concluded that CKI $\epsilon/\delta$ -dependent phosphorylation of the

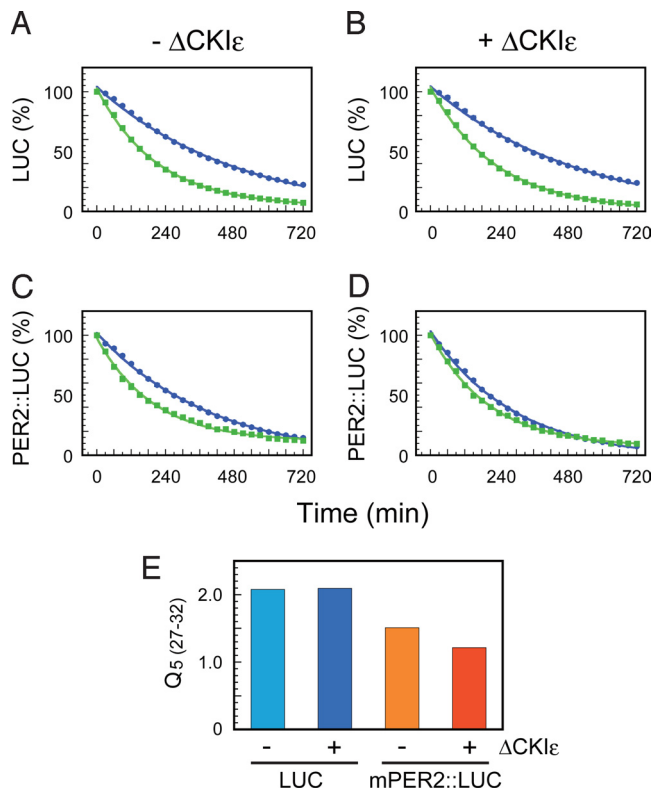


**Fig. 4.** Expression of full-length mPER2 and a catalytic domain of CKI $\epsilon$  in NIH 3T3 cells recapitulates the temperature-insensitive reaction. (A–D) Temperature dependency of decay of LUC (A and B) or mPer2::LUC (C and D) bioluminescence in NIH 3T3 cells. NIH 3T3 cells, transfected with reporter vector (pMU2-Luc or pMU2-mPer2::Luc) and an expression vector for  $\Delta$ CKI $\epsilon$  (B and D) or empty vector (A and C), were used. The degradation of LUC or mPer2::LUC was monitored after the administration of CHX to cells. The time-course data of each sample were normalized to approximate functions in which time point 0 was 100%. Each value represents the mean  $\pm$  SEM of the normalized data. The lines represent an approximated curve in which  $y = 100$  at time = 0 and  $y = 50$  at the averaged half-life time. Blue dots and line indicate the data at 27 °C; and green, 32 °C ( $n = 6$ –11). (E)  $Q_5$  values (the ratio between 27 and 32 °C) of the degradation rate of LUC or mPER2::LUC with or without co-expression of  $\Delta$ CKI $\epsilon$ . The half-lives of LUC or mPER2::LUC in each sample were calculated as described in the *SI Materials and Methods*.

mPER2 protein, which can determine the period length of circadian oscillations in clock cells, is likely temperature-insensitive.

## Discussion

**A Period-Determining and Temperature-Insensitive Process.** We discovered a highly flexible period-lengthening response in the mammalian clock: A human clock cell's circadian period could be stretched into a circadian period (Fig. 2A and E) through chemical manipulation, probably of the CKI activity, by SP600125 and TG003. We found that the knock-down of *CSNK1E* and *CSNK1D* had strong period-lengthening effects, but that of other kinases had much weaker effects, if any (Fig. 1A–C and Fig. S2B–G). Although we cannot completely exclude the possibility that our identified compounds inhibit other enzymes involved in mammalian circadian oscillations, we reason, as a first-order approximation, that these compounds lengthen the mammalian circadian oscillation primarily by inhibiting the CKI $\epsilon$  and CKI $\delta$  enzymatic activity (see also *SI Text*).

We also found that this chemically flexible period-determination process is highly robust against temperature differences, because the degradation of endogenous mPER2,

which is regulated by CKI $\epsilon$ - or CKI $\delta$ -dependent phosphorylation, was temperature-insensitive in the living clock cells (Fig. 2D and F). We also found that temperature insensitivity was preserved even in the CKI $\epsilon$ / $\delta$ -dependent phosphorylation of a synthetic peptide derived from mPER2 in vitro (Fig. 3). Moreover, the expression of exogenous full-length mPER2 protein and the catalytic domain of CKI $\epsilon$  in NIH 3T3 cells recapitulated the temperature-insensitive reaction (Fig. 4). Based on these experimental data, we propose that CKI $\epsilon$ / $\delta$ -dependent phosphorylation is likely a temperature-insensitive period-determining process in the mammalian circadian clock. In particular, we note that this enzymatic reaction is a period-accelerating reaction in mammalian circadian clocks, because enhancing this reaction by genetic mutation leads to shortening of the circadian period (36, 40), and because pharmacological inhibition of this reaction led to lengthening of the circadian period of human clock cells from a circadian ( $\approx 24$  h) to almost circadian ( $\approx 48$  h) period.

**A Period-Accelerating and Temperature-Insensitive Reaction Is Consistent with a General Theory of Temperature Compensation.** The observed period-accelerating and temperature-insensitive reaction is consistent with the previously proposed general theory for the temperature compensation of circadian clocks (41). In 1957, Sweeney and Hastings proposed that the temperature insensitivity of the primary period-determining reaction might be achieved through a balance between multiple, counteracting chemical reactions (8). This balance idea, which was mathematically formulated and generalized by Ruoff in 1992 into the balance theory (41), describes a system in which there is a balance between period-accelerating and period-decelerating reactions that yields the temperature-compensated circadian oscillation. In detail, if the period-accelerating and period-decelerating reactions were equally sensitive to temperature, the circadian oscillation would get faster with an increase in temperature. To reconcile this issue, the balance theory proposes that the period-accelerating reaction(s) are more temperature-insensitive than the period-decelerating reaction(s), and, hence, these two sets of enzymatic reactions are balanced to maintain a constant circadian oscillation. In an extreme and ideal case, the balance theory predicts that the period-accelerating reaction would be temperature-insensitive (41), which was suggested by this study.

**A Period-Accelerating and Temperature-Insensitive Reaction Is an Evolutionarily Conserved Design Principle from Cyanobacteria to Mammals.** This observed temperature insensitivity of an enzymatic reaction is the second example of such a characteristic in a circadian system. A similar temperature insensitivity was recently observed in the evolutionarily distinct cyanobacterial clock system ( $Q_{10} = \approx 1.3$  for autophosphorylation of the cyanobacteria clock protein KaiC) (24). This remarkable similarity between two very different systems implies that temperature-insensitive enzymatic reactions might represent an evolutionarily conserved design principle. We do not insist here that all individual period-determining reactions in the mammalian circadian clock are temperature-insensitive, as is observed in the cyanobacteria clock. Rather, we propose that there are some temperature-insensitive period-determining enzymatic reactions in the mammalian circadian clock, which is consistent with the balance theory. Since biochemical reactions have been believed to be highly sensitive to temperature differences for a long time, our results on the existence of temperature-insensitive reaction in vitro and in cellulo, with possible implications for temperature compensation of circadian clocks, suggest the surprising capability of CKI $\epsilon$ / $\delta$ -dependent phosphorylation. Therefore, remaining challenges are to obtain the atomic resolution model of this temperature-insensitive reaction, as well as to

demonstrate the physiological relevance of this temperature-insensitive reaction in circadian temperature compensation. Our *in vitro* temperature-insensitive reaction system, consisting of a short peptide,  $\beta$ TrCP-peptide, and a monomeric enzyme, CKI $\epsilon$  or CKI $\delta$ , would be an ideal experimental platform, which will provide atomic and molecular information required to test the physiological relevance of this temperature-insensitive reaction in circadian temperature compensation.

## Materials and Methods

**Analysis of the Effects of Compounds on Period Length in Cultured Cells.** NIH 3T3-*mPer2-Luc* cells and U2OS-*hPer2-Luc* cells were cultured on 24-well (PerkinElmer), 96-well, or 384-well (Falcon) culture plates in medium supplemented with 200  $\mu$ M luciferin (Promega) and a chemical compound with stimulation with 10 nM forskolin (Nacalai Tesque). The time-course bioluminescence data were analyzed as reported previously (42).

**Analysis of the Temperature Sensitivity of mPER2 Degradation in the *mPer2<sup>LUC</sup>* MEFs.** The *mPer2<sup>LUC</sup>* MEFs cultures were maintained on 24-well culture plate at 27, 32, or 37 °C for 4 days, and the bioluminescence from the cells was monitored by the PMT-Tron system until the oscillations of the bioluminescence from mPER2::LUC triggered by the temperature change were diminished. The cells were then treated with 400  $\mu$ g/mL CHX. The bioluminescence was recorded every 30 min for 5 h by the PMT-Tron system. The time course of the bioluminescence in each well was normalized and analyzed as described for the degradation rate of the LUC::mPER2 protein in 293T cells (SI Text).

**Measurement of CKI $\epsilon$  and CKI $\delta$  Enzymatic Activity.** CKI activity was measured by the IMAP assay using the IMAP Screening Express kit (Molecular Devices), according to the manufacturer's protocol. For the P81 phosphocellulose paper

assay, the full-length CKI $\epsilon$  and CKI $\delta$ , the catalytic domain of CKI $\epsilon$ , CKI $\delta$ , and the tau-mutant of CKI $\epsilon$  [ $\Delta$ CKI $\epsilon$ ,  $\Delta$ CKI $\delta$ ,  $\Delta$ CKI $\epsilon$  (*tau*)], and a mutant in which the eight autophosphorylated serine residues in the C-terminal regulatory domain were replaced with glutamate [CKI $\epsilon$ (D8)] purified from bacterial lysate were used as the enzymes in this assay.

**Analysis of Temperature Sensitivity of mPER2 or LUC Degradation in NIH 3T3 Cells.** NIH 3T3 cells were transfected with reporter vector (pMU2-*mPer2::Luc* or pMU2-*Luc*) and pMU2- $\Delta$ CKI $\epsilon$ (wt) or empty pMU2 using FuGene6. The transfected cells were harvested by trypsin and plated on 24-well culture plates 24 h after transfection, and the degradation of mPER2::LUC or LUC was measured as described above for *mPer2<sup>LUC</sup>* MEFs.

**ACKNOWLEDGMENTS.** We thank K. Inoue, Y. Takamiya, S. Yoshimura, K. Torii, N. Esumi, and other staff members of the Animal Resource Unit, RIKEN CDB, for the care of transgenic animals; H. Omori and Y. Uehara, Research Group for Super Analyzer Development Technology, ASI, RIKEN, for help with the construction of the CCD-Tron system; A. Taya for technical support; J.E. Baggs for technical information about gene knockdown studies using siRNA; Y. Koyama for valuable comments; J.B. Hogenesch and E.A. Kuld for valuable comments and critical reading of the manuscript; C. Johnson and M. Rosbash for information about the historical work on temperature-compensation and for suggestions for experiments; and S. Onami, the Developmental Systems Modeling Team, ASI, RIKEN, for total support. This research was supported by the National Project on Protein Structural and Functional Analyses (RIKEN), Grant-in-Aid for Scientific Research on "Development of Basic Technology to Control Biological Systems Using Chemical Compounds" from the New Energy and Industrial Technology Organization (NEDO) (to H.R.U.), Genome Network Project grant (to H.R.U.) from the Japanese Ministry of Education, Culture, Sports, Science and Technology, an intramural Grant-in-Aid from the RIKEN Center for Developmental Biology (CDB), Director's Fund from CDB (to H.R.U.), and intramural budget from the Genomic Science Center (to T.K.), and CDB (to H.R.U.), RIKEN; and National Institutes of Health Grant P50 MH074924 (to J.S.T.). J.S.T. is an Investigator in the Howard Hughes Medical Institute.

- Reppert SM, Weaver DR (2002) Coordination of circadian timing in mammals. *Nature* 418:935–941.
- Lowrey PL, Takahashi JS (2004) Mammalian circadian biology: Elucidating genome-wide levels of temporal organization. *Annu Rev Genomics Hum Genet* 5:407–441.
- Dunlap JC, Loros JJ, DeCoursey PJ, eds (2004) *Chronobiology: Biological Timekeeping* (Sinauer Associates, Sunderland, MA).
- Aschoff J (1960) Exogenous and endogenous components in circadian rhythms. *Cold Spring Harb Symp Quant Biol* 25:11–28.
- Aschoff J (1965) in *Circadian Clocks*, eds Aschoff J (North-Holland, Amsterdam), pp 95–111.
- Aschoff J (1999) Masking and parametric effects of high-frequency light-dark cycles. *Jpn J Physiol* 49:11–18.
- Pittendrigh CS (1954) On temperature independence in the clock system controlling emergence time in *Drosophila*. *Proc Natl Acad Sci USA* 40:1018–1029.
- Hastings JW, Sweeney BM (1957) On the mechanism of temperature independence in a biological clock. *Proc Natl Acad Sci USA* 43:804–811.
- Young MW, Kay SA (2001) Time zones: A comparative genetics of circadian clocks. *Nat Rev Genet* 2:702–715.
- Kondo T, et al. (1993) Circadian rhythms in prokaryotes: Luciferase as a reporter of circadian gene expression in cyanobacteria. *Proc Natl Acad Sci USA* 90:5672–5676.
- Tsuchiya Y, Akashi M, Nishida E (2003) Temperature compensation and temperature resetting of circadian rhythms in mammalian cultured fibroblasts. *Genes Cells* 8:713–720.
- Izumo M, Johnson CH, Yamazaki S (2003) Circadian gene expression in mammalian fibroblasts revealed by real-time luminescence reporting: Temperature compensation and damping. *Proc Natl Acad Sci USA* 100:16089–16094.
- Loros JJ, Feldman JF (1986) Loss of temperature compensation of circadian period length in the *frq-9* mutant of *Neurospora crassa*. *J Biol Rhythms* 1:187–198.
- Liu Y, Garceau NY, Loros JJ, Dunlap JC (1997) Thermally regulated translational control of FRQ mediates aspects of temperature responses in the *Neurospora* circadian clock. *Cell* 89:477–486.
- Ruoff P, Loros JJ, Dunlap JC (2005) The relationship between FRQ-protein stability and temperature compensation in the *Neurospora* circadian clock. *Proc Natl Acad Sci USA* 102:17681–17686.
- Dierfellner A, et al. (2007) Long and short isoforms of *Neurospora* clock protein FRQ support temperature-compensated circadian rhythms. *FEBS Lett* 581:5759–5764.
- Konopka RJ, Benzer S (1971) Clock mutants of *Drosophila melanogaster*. *Proc Natl Acad Sci USA* 68:2112–2116.
- Gekakis N, et al. (1995) Isolation of timeless by PER protein interaction: Defective interaction between timeless protein and long-period mutant PERL. *Science* 270:811–815.
- Huang ZJ, Curtin KD, Rosbash M (1995) PER protein interactions and temperature compensation of a circadian clock in *Drosophila*. *Science* 267:1169–1172.
- Rutila JE, et al. (1996) The *timS* mutant of the *Drosophila* rhythm gene *timeless* manifests allele-specific interactions with period gene mutants. *Neuron* 17:921–929.
- Matsumoto A, Tomioka K, Chiba Y, Tanimura T (1999) *timrit* Lengthens circadian period in a temperature-dependent manner through suppression of PERIOD protein cycling and nuclear localization. *Mol Cell Biol* 19:4343–4354.
- Sawyer LA, et al. (1997) Natural variation in a *Drosophila* clock gene and temperature compensation. *Science* 278:2117–2120.
- Zimmerman WF, Pittendrigh CS, Pavlidis T (1968) Temperature compensation of the circadian oscillation in *Drosophila pseudoobscura* and its entrainment by temperature cycles. *J Insect Physiol* 14:669–684.
- Tomita J, Nakajima M, Kondo T, Iwasaki H (2005) No transcription-translation feedback in circadian rhythm of KaiC phosphorylation. *Science* 307:251–254.
- Nakajima M, et al. (2005) Reconstitution of circadian oscillation of cyanobacterial KaiC phosphorylation *in vitro*. *Science* 308:414–415.
- Liu AC, Lewis WG, Kay SA (2007) Mammalian circadian signaling networks and therapeutic targets. *Nat Chem Biol* 3:630–639.
- Hirota T, et al. (2008) A chemical biology approach reveals period shortening of the mammalian circadian clock by specific inhibition of GSK-3 $\beta$ . *Proc Natl Acad Sci USA* 105:20746–20751.
- Meng QJ, et al. (2008) Setting clock speed in mammals: The CK1 $\epsilon$ psilontau mutation in mice accelerates circadian pacemakers by selectively destabilizing PERIOD proteins. *Neuron* 58:78–88.
- Tamaru T, et al. (2009) CK2 $\alpha$  phosphorylates BMAL1 to regulate the mammalian clock. *Nat Struct Mol Biol* 16:446–448.
- Maier B, et al. (2009) A large-scale functional RNAi screen reveals a role for CK2 in the mammalian circadian clock. *Genes Dev* 23:708–718.
- Bain J, et al. (2007) The selectivity of protein kinase inhibitors: A further update. *Biochem J* 408:297–315.
- Iurisci I, et al. (2006) Improved tumor control through circadian clock induction by Seliciclib, a cyclin-dependent kinase inhibitor. *Cancer Res* 66:10720–10728.
- Fabian MA, et al. (2005) A small molecule-kinase interaction map for clinical kinase inhibitors. *Nat Biotechnol* 23:329–336.
- Eide EJ, et al. (2005) Control of mammalian circadian rhythm by CK1 $\epsilon$ psilontau-regulated proteasome-mediated PER2 degradation. *Mol Cell Biol* 25:2795–2807.
- Rivers A, Gietzen KF, Vielhaber E, Virshup DM (1998) Regulation of casein kinase I epsilon and casein kinase I delta by an *in vivo* futile phosphorylation cycle. *J Biol Chem* 273:15980–15984.
- Gallego M, et al. (2006) An opposite role for tau in circadian rhythms revealed by mathematical modeling. *Proc Natl Acad Sci USA* 103:10618–10623.
- Gietzen KF, Virshup DM (1999) Identification of inhibitory autophosphorylation sites in casein kinase I epsilon. *J Biol Chem* 274:32063–32070.
- Gallego M, Virshup DM (2007) Post-translational modifications regulate the ticking of the circadian clock. *Nat Rev Mol Cell Biol* 8:139–148.
- Toh KL, et al. (2001) An hPer2 phosphorylation site mutation in familial advanced sleep phase syndrome. *Science* 291:1040–1043.
- Lowrey PL, et al. (2000) Positional syntenic cloning and functional characterization of the mammalian circadian mutation tau. *Science* 288:483–492.
- Ruoff P (1992) Introducing temperature-compensation in any reaction kinetic oscillator model. *J Interdiscipl Cycle Res* 23:92–99.
- Ukai H, et al. (2007) Melanopsin-dependent photo-perturbation reveals desynchronization underlying the singularity of mammalian circadian clocks. *Nat Cell Biol* 9:1327–1334.

**Table S3. Ten potent chemical compounds that markedly (> 10 s.d.) altered the period length in both mouse NIH3T3 and human U2OS clock cells**

Abbreviated Name <sup>a</sup>	Name <sup>b</sup>	Structure <sup>c</sup>	Function <sup>d</sup>
Roscovitine <sup>e</sup>	(R)-2-(1-Ethyl-2-hydroxyethylamino)-6-benzylamino-9-isopropylpurine		Potent, selective inhibitor of cyclin-dependent kinases (Cdc2, Cdk2 and Cdk5, but not Cdk4 or Cdk6) (24)
TG003 <sup>e</sup>	(Z)-1-(3-Ethyl-5-methoxy-2,3-dihydrobenzothiazol-2-ylidene)propan-2-one		Potent, specific, and reversible Cdc2-like kinase (Clk) inhibitor. Competes with ATP. Highly potent for Clk1 and Clk4, less for Clk2, and not effective for Clk3 (25)
SB202190 <sup>e</sup>	4-[4-(4-Fluorophenyl)-5-(4-pyridinyl)-1H-imidazol-2-yl]phenol		Highly selective, potent and cell permeable inhibitor of p38 MAP kinase alpha and beta (26)
PD169316 <sup>e</sup>	4-(4-Fluorophenyl)-2-(4-nitrophenyl)-5-(4-pyridyl)-1H-imidazole		Potent, cell-permeable, and selective p38 MAP kinase inhibitor (27)
SU5416 <sup>e</sup>	1,3-Dihydro-3-[(3,5-dimethyl-1H-pyrrol-2-yl)methylene]-2H-indol-2-one		Potent and selective vascular endothelial growth factor (VEGF) receptor protein tyrosine kinase 1/2 inhibitor (28)
DRB <sup>e</sup>	5,6-Dichlorobenzimidazole riboside		Inhibitor of Casein Kinase 2 (29) and CK2-dependent RNA synthesis
SP600125 <sup>e</sup>	Anthrapyrazolone; 1,9-Pyrazoloanthrone		Selective c-Jun N-terminal kinase (c-JNK) inhibitor. Effective for all family members of JNK (26)
CGS-15943 <sup>f</sup>	9-Chloro-2-(2-furyl)[1,2,4]triazolo[1,5-c]quinazolin-5-amine		Highly potent, non-selective adenosine receptor antagonist that binds to human A1, A2, or A3 subtypes but not to rat A3 (30, 31)
PPT <sup>g</sup>	1,3,5-tris(4-hydroxyphenyl)-4-propyl-1H-pyrazole		Specific estrogen receptor alpha (ERα) agonist. No inhibition to ERβ (32)
17-OHP <sup>g</sup>	17alpha-Hydroxyprogesterone		Metabolite of progesterone. It binds to membrane progesterone receptor (33) as well as nuclear progesterone receptor (34)

The abbreviated name (i.e. the one used in this manuscript) (a), name (b), structure (c) and short summary of its function (d) are indicated. These compounds primarily target protein kinase (e), GPCR (f) and steroid hormone receptor (g).

**Table S4** The "effective" chemical compounds that significantly (> 3 s.d. or < - 3 s.d.) alter the period-length of both mouse and human clock cells.

Name <sup>a</sup>	Structure Name <sup>b</sup>	Function <sup>c</sup>
Amsacrine hydrochloride	4-(9-Acridinylamino)-N-(methanesulfonyl)-m-anisidine hydrochloride	DNA topoisomerase II inhibitor (35)
Ketoconazole	cis-1-Acetyl-4-[4-[[2-(2,4-dichlorophenyl)-2-(1H-imidazol-1-yl)methyl]-1,3-dioxolan-4-yl]methoxy]phenyl]-piperazine	Potent inhibitor of cytochrome P450c17 enzyme; antifungal agent (36)
Picrotoxin		GABA-C receptor antagonist; powerful, nonspecific CNS stimulant isolated from Anamirta cocculin (37)
SB 216763	3-(2,4-Dichlorophenyl)-4-(1-methyl-1H-indol-3-yl)-1H-pyrrole-2,5-dione	Potent, selective, cell permeable inhibitor of glycogen synthetase kinase-3 (GSK-3) (38)
BP 897	N-[4-(4-(2-methoxyphenyl)piperazinyl)butyl]-2-naphthamide	Partially selective D3 dopamine receptor agonist (39)
9-Cp-Ade	9-cyclopentyladenine	Cell-permeable, non-competitive adenylyl cyclase inhibitor; targets the P-site domain (40)
2-Chloroadenosine	6-Amino-2-chloropurine riboside	Adenosine receptor agonist with selectivity for A1 over A2 (41)
Cyproterone acetate	6-Chloro-1beta,2beta-dihydro-17-hydroxy-3'H-cyclopropano(1,2)-pregna-1,4,6-triene-3,20-dione acetate	Androgen antagonist; synthetic steroid (42)
Chloro-IB-MECA	2-Chloro-N6-(3-iodobenzyl)-adenosine-5'-N-methyluronamide	A3 adenosine receptor agonist (43)
(R,R)-cis-Diethyl tetrahydro-2,8-chrysenediol	(5R, 11R)-5,11-Diethyl-5,6,11,12-tetrahydro-2,8-chrysenediol	Potent estrogen receptor beta antagonist; potent partial agonist at estrogen receptor alpha (44)
cis-(Z)-Flupenthixol dihydrochloride	(Z)-4-[3-[2-(Trifluoromethyl)-9H-thioxanthen-9-ylidene]propyl]-1-piperazine-ethanol dihydrochloride	Dopamine receptor antagonist; antipsychotic (45)
IB-MECA	1-Deoxy-1-[6-[[3-iodophenyl)methyl]amino]-9H-purin-9-yl]-N-methyl-beta-D-ribofuranuronamide	Selective A3 adenosine receptor agonist (43)
IIK7	N-Butanoyl 2-(9-methoxy-6H-isoindolo[2,1-a]indol-11-yl)ethanamine	Melatonin receptor agonist (46)
Phenamill methanesulfonate	3,5-Diamino-6-chloro-N-[imino(phenylamino)methyl]-pyrazinecarboxamide methansulfonate	Irreversible inhibitor of amiloride-sensitive Na <sup>+</sup> channels; derivative of amiloride (47)
SB206553 hydrochloride	N-3-Pyridinyl-3,5-dihydro-5-methyl-benzo[1,2-b:4,5-b']dipyrrole-1(2H)-carboxamide hydrochloride	Potent 5-HT2C/5-HT2B serotonin receptor antagonist (48)
Trequinsin hydrochloride	HL 725	Phosphodiesterase III (PDE III) inhibitor (49)
CGP 57380	N3-(4-fluorophenyl)-1h-pyrazolo[3,4-d]pyrimidine-3,4-diamine	Cell-permeable, selective mitogen-activated protein kinase-interacting kinase 1 (MNK1) inhibitor (50)
(R)-(+)-WIN 55,212-2 mesylate	(R)-(+)-[2,3-Dihydro-5-methyl-3[(morpholinyl)methyl]pyrrolo[1,2,3-de]-1,4-benzoxazinyl]-(1-naphthalenyl)methanone mesylate	High affinity cannabinoid receptor agonist (51)

The alias (Name) (a), structure name (b), and shortly summarized functions of the compounds (c) are listed. The upper four compounds colored gray are those that shortened the period, and the others that lengthened the period. See also **Table S3**, in which "potent effective" compounds that markedly (> 10 s.d.) alter the period-length of both clock cells are also listed.

# Supporting Information

Isojima et al. 10.1073/pnas.0908733106

## SI Text

**Detailed Procedures of the Screenings of Chemical Compounds That Affect the Period Length Both in Mouse and Human Clock Cells.** As described in the main text, we examined 1,260 pharmacologically active chemical compounds from the LOPAC<sup>1280</sup> library (Sigma-Aldrich) (1). We first screened this library with relatively high concentrations (25  $\mu\text{M}$  for NIH 3T3-*mPer2-Luc* and 50  $\mu\text{M}$  for U2OS-*hPer2-Luc*) to reduce false negatives. We found 253 compounds for NIH 3T3-*mPer2-Luc* cells and 294 compounds for U2OS-*hPer2-Luc* cells that either altered the period length by more than 3 s.d. from the negative control or induced apparent arrhythmicity. The intersection of these data yielded 166 compounds: Six and 40 compounds that shortened and lengthened, respectively, the period length of both cell types, and 120 compounds that induced apparent arrhythmicity (including compounds that were potentially cytotoxic or could affect the LUC readout) in both cell types (Table S1).

To confirm the efficacy of the 166 compounds selected above, and to exclude potentially cytotoxic or LUC-readout altering compounds, we conducted dose-dependency assays using the two clock cell lines. Three concentrations of each compound were tested for period-altering effects of approximately one order of magnitude from the concentration used in the primary assay (25, 8.3, and 2.8  $\mu\text{M}$  for NIH 3T3-*mPer2-Luc*; and 50, 16.7, and 5.6  $\mu\text{M}$  for U2OS-*hPer2-Luc*). If the lowest concentration of a compound induced an apparent arrhythmicity in the cells, two additional decreases in concentration were tested (0.93 and 0.31  $\mu\text{M}$  for NIH 3T3-*mPer2-Luc*; 1.9 and 0.62  $\mu\text{M}$  for U2OS-*hPer2-Luc*). This experiment identified nine compounds that significantly shortened ( $<-3$  s.d.) and 30 that significantly lengthened ( $>+3$  s.d.) the period length of NIH 3T3-*mPer2-Luc* cells, and seven and 90 compounds that shortened and lengthened, respectively, the period length of U2OS-*hPer2-Luc* cells (Table S2). After integrating these data across the cell types, we found four and 24 compounds that respectively shortened and lengthened the period of both cell lines. We designated these 28 compounds as “effective” compounds, and we believe they will be a useful chemical resource for circadian biology (Table S3 and Table S4). We further examined these compounds to find those with the “potent” effects ( $>+10$  s.d. or  $<-10$  s.d.,  $\approx 2.0$ – $3.0$  h) as described in the main text.

**Chemical Landscape of Period Determination in Mammalian Circadian Clocks.** As described in the main text, a chemical-biological approach was recently proposed to help elucidate the basic processes underlying circadian clocks (2). Working on a relatively small scale, previous studies revealed that several protein kinase inhibitors [such as IC261 (3, 4), CKI-7 (5), lithium chloride (6, 7), SP600125 (4, 8), and SB203580 (9)], adenylate cyclase inhibitors [such as THFA (9-tetrahydro-2-furyl-denine), 2′5′-dideoxyadonose, and 9-cyclopentyladenine (4)], and proteasome inhibitors [such as MG132 and lactacystin (3)], can lengthen the period of mammalian circadian clocks by 2% to  $\approx 40\%$ . Moreover, high-throughput screening of a large chemical compound library (1) supported using a chemical-biological approach to probe the fundamental processes of the mammalian circadian clock.

This study presents a chemical-biological approach to controlling, analyzing, and exploring the period-determination processes in the mammalian circadian clock. Using this approach, we identified 28 chemical compounds that significantly ( $>3$  s.d.) altered the period length of both human and mouse clock cell

lines (Table S3 and Table S4). Among them, 10 “potent” compounds markedly ( $>10$  s.d.) lengthened the period (Fig. S1 A and D), and lengthened it in both peripheral clock cells (MEFs) and central clock tissues (SCN) (Fig. S1 B, C, and E). These results suggest that our protocol, which featured a high-throughput chemical screening strategy and multiple cell lines of different origin [NIH 3T3 and U2OS cells were derived from NIH/Swiss mouse embryo cultures (10) and from human osteocarcinoma cells (11), respectively], and which applied a stringent threshold for “potency,” enabled the identification of exceptionally potent chemical probes that target fundamental processes in mammalian circadian clocks. By probing this “chemical landscape,” we uncovered “potent,” “effective,” and even “ineffective” compounds, which will serve as a useful guide for drug researchers seeking cures for rhythm disorders.

So far, this chemical landscape features at least two salient landmarks: One is the period-determining process targeted by 17-OHP and the other is the period-determining process targeted by CKI $\epsilon/\delta$  activity. Since progesterone and progestins, synthetic progesterone derivatives such as 17-hydroxyprogesterone caproate and medroxyprogesterone, are widely available as clinical drugs (12), the 17-OHP “landmark” serves as a good vantage point for putative therapeutics (Fig. S1) to mitigate rhythm disorders such as advanced sleep phase syndrome (ASPS) (i.e., via an agonist like 17-OHP). While guiding drug discovery, the landmarks on this revealing chemical landscape will also be useful for further exploration of the fundamental properties of mammalian circadian clocks.

**Validity of Relatively Higher-Dose Applications of Potent Effective Compounds in Vitro and in Cellulo.** In this chemical-biological study, we discovered a highly flexible period-lengthening response in the mammalian clock: A human clock cell’s circadian period could be stretched into a circadian period (Fig. 2A) through chemical manipulation, probably of the CKI activity, by SP600125 and TG003. The half-maximum concentrations of these compounds for their period-lengthening effect in cellulo were  $\approx 22$  and 63  $\mu\text{M}$ , respectively. In contrast, the IC<sub>50</sub>s of SP600125 and TG003 for the CKI $\epsilon$  kinase activity with 20  $\mu\text{M}$  ATP in vitro were  $\approx 0.22$  and 0.55  $\mu\text{M}$ , respectively (Fig. 1E). If these compounds function as competitive inhibitors for ATP, this apparent discrepancy can be largely explained by the difference in ATP concentration, which is  $\approx 1$  mM inside cells (13–15). This competitive-inhibition hypothesis is experimentally supported by our observations that higher amounts of inhibitors were required in assays with a high concentration of ATP (100  $\mu\text{M}$  ATP; Fig. 1D) than with a lower concentration (20  $\mu\text{M}$  ATP; Fig. 1E). Given that the Michaelis constant for ATP with CKI $\epsilon$  is  $\approx 20$   $\mu\text{M}$ , the ratio of the IC<sub>50</sub> with 1 mM ATP (in cellulo) to that with 20  $\mu\text{M}$  ATP (in vitro kinase assay) is 25.5, and hence the IC<sub>50</sub>s of SP600125 and TG003 with 1 mM ATP should be  $\approx 5.6$  and 14.5  $\mu\text{M}$ , respectively. Although there is still a 4-fold difference between the half-maximum concentrations in cellulo and the estimated IC<sub>50</sub>s with 1 mM ATP, these values are within the same order of magnitude. The difference might be owing to the dynamics of these compounds in cellulo, such as the efficiency of their penetration into cells, nonspecific buffering by other proteins within cells, and excretion from cells. Another possibility is that these potent compounds act on other targets in addition to CKI $\epsilon$  and CKI $\delta$ , such as their “primary” targets, which might be strongly involved in the period-determining processes of mammalian circadian clocks. However, the latter

possibility was not supported by the results of our siRNA experiments, in which we knocked down kinases including the “primary” targets of the potent compounds (Fig. S2).

**Temperature-Insensitivity of CKI Phosphorylation Depended on the Substrate Recognition.** CKIs recognize the motif “Ser/Thr-x-x-Ser/Thr,” and phosphorylate the Ser/Thr residue at the C-terminal end. Negative charge at the N-terminal end of the motif was thought to be the “priming signal” of the CKI-dependent phosphorylation, because phosphorylation of the Ser/Thr residue at the N-terminal end or replacement of the residue to the acidic amino acid (Glu or Asp) remarkably improved the efficiency of the CKI-dependent phosphorylation (16). As described in the main text, phosphorylation of  $\beta$ TrCP peptide or FASPS-peptide by  $\Delta$ CKI $\epsilon$ (wt) were relatively temperature-insensitive ( $\beta$ TrCP;  $Q_{10} = 1.0$ , FASPS;  $Q_{10} = 1.2$ ), although that of CK1tide was more temperature-sensitive (CK1tide;  $Q_{10} = 1.4$ ) (Fig. 3). It should be noted that the CK1tide was “primed,” but the former two substrates were not. Moreover, the *tau* mutation (R178C) of CKI $\epsilon$ , which are thought to affect substrate recognition of CKI $\epsilon$ , resulted to become temperature-sensitive in the phosphorylation of the FASPS-peptide ( $Q_{10} = 1.6$ ). These results implied that substrate recognition by CKI $\epsilon/\delta$  was a crucial process for defining temperature-dependency of CKI $\epsilon/\delta$ -dependent phosphorylation. We also noted that priming phosphorylation at a Ser-662 residue of hPER2, associating with FASPS, was regulating protein stability and nuclear translocation or transcriptional repressor activity, although a kinase responsible for the priming phosphorylation have not been identified (17).

## SI Materials and Methods

**Establishment of a High-Throughput Screening System Using a Cooled CCD-Camera (CCD-Tron System).** To perform high-throughput screening of a chemical compound library, we developed a screening system that uses a high-performance CCD camera, based on a monitoring system using photomultiplier tubes (PMT) described in a previous report (PMT-Tron system) (18). The round turntable (Mashinax or NEXSYS Corp.) enables the observation of up to 12 culture plates at once, and thus 4,608 samples can be screened simultaneously if 384-well culture plates are used. The computer-controlled turntable rotates and sequentially sets each of the plates under the CCD camera every 5 min. The bioluminescence from the culture plate is imaged by the high-performance CCD camera (VersArray XP or PIXIS; Roper Scientific). The intensity of each well is calculated from the obtained image by a custom-made computer program

**Establishment of Stable Transfectants of NIH 3T3 Cells Expressing the *mPer2-Luc* Reporter.** The mouse *Per2* promoter-driven reporter plasmid (*mPer2-Luc*) (19) and the pIRESHyg3 plasmid (BD Biosciences) were cotransfected into NIH 3T3 cells with FuGene6 transfection reagent (Roche). NIH 3T3 clones expressing *mPer2-Luc* (NIH 3T3-*mPer2-Luc*) were selected using 200  $\mu$ g/mL hygromycin B (Invitrogen).

**Establishment of Stable Transfectants of U2OS Cells Expressing the *hPer2-Luc* Reporter.** A 334-bp fragment of the human *Per2* gene promoter, 502- to 169-bp upstream from exon 1, was amplified by PCR with PrimeSTAR DNA polymerase (TaKaRa) and the following primers:

F: 5'-GGGGTACCAGGGCGTAGTGAATGGAAG-3'

R: 5'-CCCAAGCTTAGCTGCACGTATCCCCCTCAG-3'

This promoter fragment was subcloned into the reporter vector, pGL4.14 (Promega) with the restriction enzymes, *Kpn*I and *Hind*III (TaKaRa). This *hPer2* promoter-driven reporter plasmid (*hPer2-Luc*) was transfected into U2OS cells (purchased from American Type of Culture Collections; ATCC), and stable

transfectants (U2OS-*hPer2-Luc*) were selected as described for the NIH 3T3 cells.

**Preparation of Embryonic Fibroblasts from *mPer2<sup>Luc</sup>* Mice.** The *mPer2<sup>Luc</sup>* mice (20) were carefully kept and handled according to the RIKEN Regulations for Animal Experiments. Embryos of *mPer2<sup>Luc</sup>* mice at E13  $\approx$  15 were excised and washed several times with Hanks' balanced salt solution. After the placenta and internal organs were completely removed, the embryos were cut into small pieces, and the cells were dissociated by incubation in 0.05% trypsin solution with 0.53 mM EDTA for 30 min at 37 °C. The dissociated cells (mouse embryonic fibroblasts from *mPer2<sup>Luc</sup>* mice; *mPer2<sup>Luc</sup>* MEFs) were suspended and cultured in the growth medium (DMEM supplemented with 10% FBS).

**Preparation of SCN Slices from *mPer2<sup>Luc</sup>* Mice.** The brains were removed from quickly decapitated, young (older than 4 weeks of age) *mPer2<sup>Luc</sup>* mice, then 300- $\mu$ m-thick coronal sections containing the SCN were made using a vibratome type linearslicer (PRO7; Dosaka EM Corp) in ice cold Hanks' balanced salt solution (Invitrogen). The slices were then placed on a culture membrane (MilliCell-CM; Millipore) and set on a dish with 1.2 mL culture medium [DMEM supplemented with 1.2 g/L NaHCO<sub>3</sub> (Nacalai Tesque), 15 mM HEPES (Dojindo), 20 mg/L kanamycin (Invitrogen), 5  $\mu$ g/mL insulin (Sigma), 20 nM putrescine (Sigma), 100  $\mu$ g/mL apo-transferrin (Sigma), 20 nM progesterone (Sigma), 30 nM sodium selenite (Sigma), one-fiftieth part B-27 supplement (Invitrogen), and 100  $\mu$ M luciferin] containing the chemical compounds at the concentrations indicated in Fig. S1C.

**Analysis of the Effects of Compounds on Period Length in Cultured Cells and Slices.** NIH 3T3-*mPer2-Luc* cells, U2OS-*hPer2-Luc* cells, and *mPer2<sup>Luc</sup>* MEFs were cultured on 24-well (PerkinElmer), 96-well, or 384-well (Falcon) culture plates, and 300  $\mu$ m-thick coronal slices containing the SCN from *mPer2<sup>Luc</sup>* mice on a culture membrane (MilliCell-CM; Millipore) in medium supplemented with 200  $\mu$ M luciferin (Promega) and a chemical compound with (cells) or without (slices) stimulation with 10 nM forskolin (Nacalai Tesque). The culture plates were placed in a high-sensitivity bioluminescence detection system (LM-2400; Hamamatsu Photonics, for slices; PMT-Tron for MEFs; or CCD-Tron, for others), and the bioluminescence of each well was measured at 30 °C (cells) or 37 °C (slices) (Fig. S1 D and E). The time-course bioluminescence data were analyzed as reported previously (18).

**Rhythmicity and Period Length Analysis of Real-Time Bioluminescence Data.** The rhythmicity and period length were determined from the bioluminescence data of NIH 3T3-*mPer2-Luc* cells, U2OS-*hPer2-Luc* cells, MEFs, and SCN slices, as previously reported (18). Although this method could not be used for samples with a period length longer than 36 h, we modified the analysis method to examine the long periods of circadian clocks in the presence of high concentrations of potent period-lengthening compounds (TG003 and SP600125) (Fig. 2A). The data obtained 36 h after the addition of forskolin and compound, instead of 21 h, were used for analysis to eliminate the first cycle, and detrending was performed not to detect the periodicity longer than 72 h, instead of 42 h in usual method. These modifications enabled us to examine periodicities up to 56 h.

**Gene Knockdown Studies Using siRNA in U2OS-*hPer2-Luc* Cells.** U2OS-*hPer2-Luc* cells were plated at  $3.0 \times 10^4$  cells per well in 24-well multiwell plates, 24 h before the transfection. The predesigned *Silencer* Select siRNAs (Ambion) were transfected with Lipofectamine 2000 reagent (Invitrogen) as described in the manufacturer's protocol. At least three siRNA clones for each

gene were examined. The siRNA was used at 5 to 20 pmol/well, and the total amount of transfected siRNA was adjusted to 20 pmol/well using *Silencer Select* negative control #2 siRNA (Ambion).

A pair of culture plates was prepared for each transfection condition. The medium on one plate was changed to the recording medium containing 10 nM forskolin and 100  $\mu$ M luciferin 24 h after the transfection, placed into the PMT-Tron system, and the period length was measured as described above. The total RNA of the cells on the other plate was purified with TRIzol reagent (Invitrogen), and the cDNA was reverse-transcribed using SuperScript II or III (Invitrogen) with random primers (Invitrogen), as described in the manufacturer's protocol. The gene expression levels were quantified with the QuantiFast SYBR PCR kit (Qiagen) with a LightCycler 480 (Roche Applied Science) or PRISM 7900 HT (PerkinElmer), according to the manufacturers' protocols.

The ID numbers of the predesigned *Silencer Select* siRNAs used in these studies were as follows:

**Cry2.** s3537; *CSNK1E*: s57, s58, and s59; *CSNK1D*: s3627, s3628, and s3629; *MAPK8*: s11152, s11153, and s11154; *MAPK9*: s11158, s11159, and s11160; *CLK1*: s3162, s3163, s3164; *CLK2*: s3165, s3166, and s3167; *CLK4*: s32986, s32987, and s32988; *CDK2*: s204, s205, and s206; *CDK5*: s2825, s2826, and s2827; *CDC2*: s463, s464, and s465; *MAPK14*: s3585, s3586, and s3587; *MAPK11*: s11155, s11156, and s11157; *MAPK12*: s12467, s12468, and s12469; *CSNK2A1*: s3636, s3637, and s3638; *CSNK2A2*: s3639, s3640, and s3641; *ADORA1*: s1085, s1086, and s1087; *ADORA2A*: s1088, s1089, and s1090; *ADORA2B*: s1091, s1092, and s1093. In addition, the following custom designed *Silencer Select* siRNAs were used:

*CLK1*: s229161 and s229162; *CLK2*: s229159 and s229160; *CLK4*: s229157 and s229158.

**Expression and Purification of mCKI $\epsilon/\delta$  Protein.** Mouse *CKI $\epsilon$*  ORFs, corresponding to amino acids 2–416 (full-length *CKI $\epsilon$* ) and 2–319 ( $\Delta$ *CKI $\epsilon$* ), and *CKI $\delta$*  ORFs, corresponding to amino acids 2–415 (full-length *CKI $\delta$* ) and 2–317 ( $\Delta$ *CKI $\delta$* ), were cloned into the pGEX-6P-1 vector (GE Healthcare) and then introduced into *Escherichia coli* Rosetta2 (Novagen). A *CKI $\epsilon$*  ORF in which eight serine residues identified as autophosphorylation amino acids (21) in the C-terminal region were replaced with glutamate, referred to as *CKI $\epsilon$*  (D8), was also cloned and introduced into *E. coli*. Cells were grown at 25 °C until they reached an OD<sub>600</sub> absorbance of about 0.5. After the addition of isopropyl  $\beta$ -D-1-thiogalactopyranoside (IPTG) to a final concentration of 0.1 mM, the cells were further grown at 25 °C for 24 h. The cells were collected and resuspended in extraction buffer [50 mM Tris-HCl, pH 7.5, 300 mM NaCl, 1 mM DTT, 1 mM EDTA, 10% glycerol, and complete protease inhibitor mixture (Roche)] and homogenized by sonication. The homogenate was spun at 38,000 $\times$  g, and the supernatant was applied to a Glutathione Sepharose 4B column (GE Healthcare). The column was washed with five column volumes of the buffer. PreScission Protease (GE Healthcare) was then applied to the column to remove the GST-tag, according to the manufacturer's protocol. The proteins were eluted with two column volumes of elution buffer (50 mM Tris-HCl, pH 7.5, 300 mM NaCl, 1 mM DTT, 1 mM EDTA, and 10% glycerol), and the eluent was diluted and applied to a HiTrap SP HP column (GE Healthcare). The proteins were then eluted with 600 mM NaCl. The protein concentration was determined by the Bradford method, using the Bio-Rad Laboratories protein assay kit with BSA (Bio-Rad Laboratories) as a standard. The purified proteins used in this study are shown in Fig. S6 B and C.

**Measurement of CKI Enzymatic Activity.**  $\Delta$ *CKI $\epsilon$*  protein (0.5  $\mu$ M) was added to the reaction buffer (25 mM Tris-HCl, pH 7.5, 7.5 mM MgCl<sub>2</sub>, 1 mM DTT, 0.1 mg/mL BSA, and 200 nM synthetic peptide substrate) with different concentrations of chemicals (25, 50, or 100  $\mu$ M for the potent compounds; 100  $\mu$ M for IC261), preincubated at 30 °C for 5 min, and then the reaction was started by adding a one-fourth volume of 400  $\mu$ M ATP. Aliquots (1  $\mu$ L) of the reaction mixture were withdrawn in triplicate at 0 and 1 h of the reaction and mixed with 30  $\mu$ L IMAP binding buffer in 384-well glass-bottomed plates (Olympus). After incubating for at least 1 h at ambient temperature, the fluorescent polarization was measured using a single-molecule fluorescence detection (SMFD) system (MF20; Olympus).

The measurement of CKI kinase activity using a P81 phosphocellulose paper assay was performed as follows. Peptides consisting of 34 aa (RKKKPHSGSSGYGSLGSNG-SHEHLMSQTSSSDSN), referred to as  $\beta$ TrCP-peptide (22), and 29 aa (RKKKTEVSAHLSSLTLPKGAESVVSLSQ), referred to as FASPS-peptide, were synthesized and purchased from Bio-Synthesis Inc. CK1tide (KRRRAL[pS]VASLPGL; Upstate), and  $\alpha$ -casein from bovine milk (Sigma) were used as the substrate.

$\Delta$ *CKI $\epsilon/\delta$*  proteins (0.2  $\mu$ M for  $\beta$ TrCP-peptide and FASPS-peptide, 0.02  $\mu$ M for  $\alpha$ -casein, 0.01  $\mu$ M for CK1tide) in the reaction buffer (25 mM Tris, pH 7.5, 7.5 mM MgCl<sub>2</sub>, 1 mM DTT, 0.1 mg/mL BSA, and 200  $\mu$ M peptide substrate or 40  $\mu$ M casein) were preincubated for 5 min. The reaction was started by adding a one-fourth volume of 2 mM (Fig. S6D), 400  $\mu$ M (Fig. 1D), or 80  $\mu$ M (Fig. 1E) ATP with 0.5–1  $\mu$ Ci [ $\gamma$ -<sup>32</sup>P] ATP per reaction. In assays for autophosphorylated *CKI $\epsilon/\delta$*  (0.4  $\mu$ M for  $\beta$ TrCP-peptide, 0.04  $\mu$ M for  $\alpha$ -casein, and CK1tide), the enzyme was preincubated with buffer (25 mM Tris, pH 7.5, 7.5 mM MgCl<sub>2</sub>, 1 mM DTT, 0.1 mg/mL BSA, 500  $\mu$ M ATP) at 30 °C for 1 h, and the reaction was started by adding substrate. The preincubation and incubation steps were performed at 25 ° or 35 °C. Two aliquots (10  $\mu$ L) of the reaction mixture were withdrawn at each time point and spotted onto P81 phosphocellulose paper (Whatman) in the case of peptide substrates, or mixed with SDS-PAGE buffer for casein. The P81 phosphocellulose papers were washed five times with 75 mM orthophosphate and once with 100% EtOH, then placed in scintillation vials with scintillation mixture (AQUASOL-2; PerkinElmer). The incorporation of P<sub>i</sub> was quantified using a scintillation counter (LSC-6100; Aloka) or by autoradiography after SDS-PAGE (BAS-2500; Fuji Photo Film).

**Analysis of the Degradation Rate of mPER2 Protein in 293T, NIH 3T3, or mPer2<sup>Luc</sup> MEF Cells.** The intensity of the LUC::mPER2 from 293T cells, mPER2::LUC from NIH 3T3 cells, or mPer2<sup>Luc</sup> MEFs was normalized so that the average luminescence detected at t = 0 was defined as '100'. To calculate the half-life of LUC-fused protein, the normalized results were fitted with the equation,

$$y = ae^{-kt} + (100 - a)$$

y, normalized bioluminescence intensity; t, time after addition of cycloheximide (CHX); a, k, variables. e, Napier's constant.

And the half-life  $t_{1/2}$  was calculated as follows:

$$t_{1/2} = -\ln\left(\frac{(a - 50)}{a}\right) \frac{1}{k}.$$

**Analysis of the Temperature Sensitivity of mPER2 Degradation in the mPer2<sup>Luc</sup> MEFs.** The cultures were maintained at 27 °, 32 °, or 37 °C for 4 days, and the bioluminescence from the cells was monitored by the PMT-Tron system until the oscillations of the bioluminescence from mPER2::LUC triggered by the temperature change were diminished. The cells were then treated with 400

$\mu\text{g}/\text{mL}$  CHX. The bioluminescence was recorded every 30 min for 5 h by the PMT-Tron system. The time course of the bioluminescence in each well was normalized and analyzed as described for the degradation rate of the LUC::mPER2 protein in 293T cells.

**Construction of Expression Vectors for a Reporter Assay to Examine Clock-Related Protein Stability.** To investigate the stability of clock-related proteins (PER2, PER1, and BMAL1) in cultured 293T cells, we constructed an expression plasmid bearing the firefly Luciferase protein fused to the N-terminal end of clock-related proteins (LUC::mPER2, LUC::mPER1, and LUC::mBMAL1) under the CMV promoter (CMV-*Luc::mPer2*, CMV-*Luc::mPer1*, and CMV-*Luc::mBmal1*). We also constructed an expression vector bearing the firefly luciferase protein fused to the C-terminal end of the mouse Per2 protein (mPER2::LUC) using a custom expression vector pMU2 (18) for studies in cultured NIH 3T3 cells (pMU2-*mPer2::Luc*). The cDNAs of these clock-related proteins were kindly provided by Dr. H. Tei (Mitsubishi Kagaku Institute for Life Sciences, Japan). A control expression vector expressing the LUC protein under the CMV promoter (CMV-*Luc*) was also constructed.

The coding sequence of *mCKI $\epsilon$ (wt)* was subcloned into the pMU2 expression vector as previously described [pMU2-*mCKI $\epsilon$ (wt)*]. An expression vector for the *mCKI $\epsilon$ (tau)* mutant (in which Arg-178 was replaced with Cys) was constructed by inverse PCR using pMU2-*mCKI $\epsilon$ (wt)* as a template. Inverse PCR was performed using the following PCR primers.

F: 5'-TGCTATGCCTCTATCAACACCCAC-3'

R: 5'-GGCAGTGCCGGTCAGGTTCTTG-3' (the 5' end was phosphorylated).

Finally, self-ligation of the PCR product was performed. The resultant vector was named pMU2-*mCKI $\epsilon$ (tau)*.

An expression vector bearing only the catalytic domain of *mCKI $\epsilon$*  ( $\Delta$ mCKI $\epsilon$ ) was also constructed. The coding sequence of the regulatory domain of *mCKI $\epsilon$* , corresponding to amino acids 320 to 416, was deleted from pMU2-*mCKI $\epsilon$ (wt)* by inverse PCR. The resultant vector was named pMU2- $\Delta$ mCKI $\epsilon$ (wt).

The *mCKI $\epsilon$ (wt)*, *mCKI $\epsilon$ (tau)*, or  $\Delta$ mCKI $\epsilon$ (wt) gene was fused in-frame with 1 $\times$  Flag Tag at the N terminus, and regulated by the CMV promoter.

**Analysis of mPER2 Protein Stability in 293T Cells.** 293T cells transfected with expression vectors for LUC::mPER2, *CKI $\epsilon$ (tau)*, and *Renilla* Luciferase were subcultured on 96- or 384-well culture plates. The stability of the LUC::mPER2 protein was measured after a 24-h incubation with a chemical compound, and the degradation rate of LUC::mPER2 was determined at the indi-

cated times after adding 200  $\mu\text{g}/\text{mL}$  CHX. The LUC activity was measured using the Dual-Glo bioluminescence detection kit (Promega) following the manufacturer's protocol. The degradation rate was calculated as described above.

**Western Blot of mPER2 Protein Expressed in 293T Cells.** 293T cells, grown in DMEM supplemented with 10% FBS and antibiotics (25 U/mL penicillin, 25 mg/mL streptomycin; Invitrogen), were plated at  $4 \times 10^5$  cells per dish in 35-mm dishes. Twenty-four hours later, the cells were transfected with FuGene6 (Roche), according to the manufacturer's instructions. The cells were transfected with 2  $\mu\text{g}$  pcDNA3-*Myc-mPer2* (a gift from Dr. E. Nishida, Kyoto University) (23), 2  $\mu\text{g}$  pMU2-*mCKI $\epsilon$ (tau)*, or empty plasmid pMU2, and 2  $\mu\text{g}$  pMU2-*Luc*. After 24 h, the cells transfected with the *mCKI $\epsilon$ (tau)* expression vector were harvested, combined, and then replated onto the same number of 35-mm dishes to normalize for variations in the transfection efficiencies due to different plates. After 48 h, the cells were treated with or without 100  $\mu\text{M}$  TG003 or SP600125 in 0.2% DMSO (Nacalai Tesque). The treated cells were harvested at the times indicated in Fig. S4, lysed with the extraction reagent [50 mM Tris-HCl, pH 8.1, 10 mM EDTA, 1% SDS, Halt Protease Inhibitor Mixture, EDTA-free (Pierce)], and sonicated. The protein concentration of the samples was measured by the Bradford method using a Bio-Rad Laboratories protein assay kit (Bio-Rad Laboratories). Equal amounts of protein (0.25 mg) were then mixed with NuPAGE LDS sample buffer (Invitrogen), and the samples were separated by electrophoresis and transferred to PVDF membranes using the NuPAGE electrophoresis system (Invitrogen), as described in the manufacturer's protocol. Myc-mPER2 protein was detected with an anti-Myc monoclonal antibody (clone A-14; Santa Cruz Biotechnology) and HRP-conjugated anti-rabbit IgG secondary antibody (GE Healthcare). An anti-tubulin $\alpha$  monoclonal antibody (clone DM1A; LAB VISION) and anti-mouse IgG secondary antibody (GE Healthcare) were used to detect tubulin $\alpha$  protein. The immunoreactivities were visualized and quantified using the ECL Plus Western Blotting Detection system (GE Healthcare) and LAS-1000 (Fujifilm), according to the manufacturers' instructions.

**Analysis of Temperature Sensitivity of mPER2 or LUC Degradation in NIH 3T3 Cells.** NIH 3T3 cells cultured on 100-mm plates were transfected with 30  $\mu\text{g}$  reporter vector (pMU2-*mPer2::Luc* or pMU2-*Luc*) and 6  $\mu\text{g}$  pMU2- $\Delta$ CKI $\epsilon$ (wt) or empty pMU2 using 60  $\mu\text{L}$  FuGene6. The transfected cells were dissociated by trypsin and plated on 24-well culture plates 24 h after transfection, and the degradation of mPER2::LUC or LUC was measured as described above for *mPer2<sup>Luc</sup>* MEFs.

- Hirota T, et al. (2008) A chemical biology approach reveals period shortening of the mammalian circadian clock by specific inhibition of GSK-3 $\beta$ . *Proc Natl Acad Sci USA* 105:20746–20751.
- Liu AC, Lewis WG, Kay SA (2007) Mammalian circadian signaling networks and therapeutic targets. *Nat Chem Biol* 3:630–639.
- Eide EJ, et al. (2005) Control of mammalian circadian rhythm by CKI $\epsilon$ -regulated proteasome-mediated PER2 degradation. *Mol Cell Biol* 25:2795–2807.
- O'Neill JS, et al. (2008) cAMP-dependent signaling as a core component of the mammalian circadian pacemaker. *Science* 320:949–953.
- Vanselow K, et al. (2006) Differential effects of PER2 phosphorylation: Molecular basis for the human familial advanced sleep phase syndrome (FASPS). *Genes Dev* 20:2660–2672.
- Abe M, Herzog ED, Block GD (2000) Lithium lengthens the circadian period of individual suprachiasmatic nucleus neurons. *Neuroreport* 11:3261–3264.
- Iwahana E, et al. (2004) Effect of lithium on the circadian rhythms of locomotor activity and glycogen synthase kinase-3 protein expression in the mouse suprachiasmatic nuclei. *Eur J Neurosci* 19:2281–2287.
- Chansard M, et al. (2007) c-Jun N-terminal kinase inhibitor SP600125 modulates the period of mammalian circadian rhythms. *Neuroscience* 145:812–823.
- Hayashi Y, et al. (2003) p38 mitogen-activated protein kinase regulates oscillation of chick pineal circadian clock. *J Biol Chem* 278:25166–25171.
- Jainchill JL, Aaronson SA, Todaro GJ (1969) Murine sarcoma and leukemia viruses: assay using clonal lines of contact-inhibited mouse cells. *J Virol* 4:549–553.
- Ponten J, Saksela E (1967) Two established in vitro cell lines from human mesenchymal tumours. *Int J Cancer* 2:434–447.
- Meis PJ (2005) 17 Hydroxyprogesterone for the prevention of preterm delivery. *Obstet Gynecol* 105:1128–1135.
- Wang RH, Tao L, Trumbore MW, Berger SL (1997) Turnover of the acyl phosphates of human and murine prothymosin alpha in vivo. *J Biol Chem* 272:26405–26412.
- Sippel CJ, Dawson PA, Shen T, Perlmutter DH (1997) Reconstitution of bile acid transport in a heterologous cell by cotransfection of transporters for bile acid uptake and efflux. *J Biol Chem* 272:18290–18297.
- Kennedy HJ, et al. (1999) Glucose generates sub-plasma membrane ATP microdomains in single islet beta-cells. Potential role for strategically located mitochondria. *J Biol Chem* 274:13281–13291.
- Flotow H, et al. (1990) Phosphate groups as substrate determinants for casein kinase I action. *J Biol Chem* 265:14264–14269.
- Xu Y, et al. (2007) Modeling of a human circadian mutation yields insights into clock regulation by PER2. *Cell* 128:59–70.
- Ukai H, et al. (2007) Melanopsin-dependent photo-perturbation reveals desynchronization underlying the singularity of mammalian circadian clocks. *Nat Cell Biol* 9:1327–1334.
- Sato TK, et al. (2006) Feedback repression is required for mammalian circadian clock function. *Nat Genet* 38:312–319.
- Yoo SH, et al. (2004) PERIOD2::LUCIFERASE real-time reporting of circadian dynamics reveals persistent circadian oscillations in mouse peripheral tissues. *Proc Natl Acad Sci USA* 101:5339–5346.

21. Gietzen KF, Virshup DM (1999) Identification of inhibitory autophosphorylation sites in casein kinase I epsilon. *J Biol Chem* 274:32063–32070.
22. Lowrey PL, et al. (2000) Positional syntenic cloning and functional characterization of the mammalian circadian mutation tau. *Science* 288:483–492.
23. Akashi M, Tsuchiya Y, Yoshino T, Nishida E (2002) Control of intracellular dynamics of mammalian period proteins by casein kinase I epsilon (CKIepsilon) and CKIdelta in cultured cells. *Mol Cell Biol* 22:1693–1703.
24. Meijer L, et al. (1997) Biochemical and cellular effects of roscovitine, a potent and selective inhibitor of the cyclin-dependent kinases cdc2, cdk2 and cdk5. *Eur J Biochem* 243:527–536.
25. Muraki M, et al. (2004) Manipulation of alternative splicing by a newly developed inhibitor of Clks. *J Biol Chem* 279:24246–24254.
26. Bain J, et al. (2007) The selectivity of protein kinase inhibitors: A further update. *Biochem J* 408:297–315.
27. Kummer JL, Rao PK, Heidenreich KA (1997) Apoptosis induced by withdrawal of trophic factors is mediated by p38 mitogen-activated protein kinase. *J Biol Chem* 272:20490–20494.
28. Fong TA, et al. (1999) SU5416 is a potent and selective inhibitor of the vascular endothelial growth factor receptor (Flk-1/KDR) that inhibits tyrosine kinase catalysis, tumor vascularization, and growth of multiple tumor types. *Cancer Res* 59:99–106.
29. Zandomeni R, Weinmann R (1984) Inhibitory effect of 5,6-dichloro-1-beta-D-ribofuranosylbenzimidazole on a protein kinase. *J Biol Chem* 259:14804–14811.
30. Ghai G, et al. (1987) Pharmacological characterization of CGS 15943A: A novel nonxanthine adenosine antagonist. *J Pharmacol Exp Ther* 242:784–790.
31. Kim YC, Ji XD, Jacobson KA (1996) Derivatives of the triazoloquinazoline adenosine antagonist (CGS15943) are selective for the human A3 receptor subtype. *J Med Chem* 39:4142–4148.
32. Kraichely DM, Sun J, Katzenellenbogen JA, Katzenellenbogen BS (2000) Conformational changes and coactivator recruitment by novel ligands for estrogen receptor-alpha and estrogen receptor-beta: Correlations with biological character and distinct differences among SRC coactivator family members. *Endocrinology* 141:3534–3545.
33. Ashley RL, et al. (2006) Cloning and characterization of an ovine intracellular seven transmembrane receptor for progesterone that mediates calcium mobilization. *Endocrinology* 147:4151–4159.
34. Baker ME, et al. (1984) Chick oviduct progesterone receptor binding of 15 beta, 17-dihydroxyprogesterone and its analogues. *Steroids* 43:153–158.
35. Nelson EM, Tewey KM, Liu LF (1984) Mechanism of antitumor drug action: Poisoning of mammalian DNA topoisomerase II on DNA by 4'-(9-acridinylamino)-methanesulfonm-aniside. *Proc Natl Acad Sci USA* 81:1361–1365.
36. Eagling VA, Tjia JF, Back DJ (1998) Differential selectivity of cytochrome P450 inhibitors against probe substrates in human and rat liver microsomes. *Br J Clin Pharmacol* 45:107–114.
37. Yoon KW, Covey DF, Rothman SM (1993) Multiple mechanisms of picrotoxin block of GABA-induced currents in rat hippocampal neurons. *J Physiol* 464:423–439.
38. Smith DG, et al. (2001) 3-Anilino-4-arylmaleimides: Potent and selective inhibitors of glycogen synthase kinase-3 (GSK-3). *Bioorg Med Chem Lett* 11:635–639.
39. Pilla M, et al. (1999) Selective inhibition of cocaine-seeking behaviour by a partial dopamine D3 receptor agonist. *Nature* 400:371–375.
40. Johnson RA, et al. (1997) Isozyme-dependent sensitivity of adenyl cyclases to P-site-mediated inhibition by adenine nucleosides and nucleoside 3'-polyphosphates. *J Biol Chem* 272:8962–8966.
41. Thompson RD, Secunda S, Daly JW, Olsson RA (1991) Activity of N6-substituted 2-chloroadenosines at A1 and A2 adenosine receptors. *J Med Chem* 34:3388–3390.
42. Kempainen JA, et al. (1999) Distinguishing androgen receptor agonists and antagonists: Distinct mechanisms of activation by medroxyprogesterone acetate and dihydrotestosterone. *Mol Endocrinol* 13:440–454.
43. Jacobson KA, et al. (1995) Structure-activity relationships of 9-alkyladenine and ribose-modified adenosine derivatives at rat A3 adenosine receptors. *J Med Chem* 38:1720–1735.
44. Meyers MJ, et al. (2001) Estrogen receptor-beta potency-selective ligands: Structure-activity relationship studies of diarylpropionitriles and their acetylene and polar analogues. *J Med Chem* 44:4230–4251.
45. Nymark M, et al. (1973) Prolonged neuroleptic effect of alpha-flupenthixol decanoate in oil. *Acta Pharmacol Toxicol (Copenh)* 33:363–376.
46. Faust R, et al. (2000) Mapping the melatonin receptor. 6. Melatonin agonists and antagonists derived from 6H-isoindolo[2,1-a]indoles, 5,6-dihydroindolo[2,1-a]isoquinolines, and 6,7-dihydro-5H-benzo[c]azepino[2,1-a]indoles. *J Med Chem* 43:1050–1061.
47. Garvin JL, Simon SA, Cragoe EJ, Jr, Mandel LJ (1985) Phenamil: An irreversible inhibitor of sodium channels in the toad urinary bladder. *J Membr Biol* 87:45–54.
48. Kennett GA, et al. (1996) In vitro and in vivo profile of SB 206553, a potent 5-HT2C/5-HT2B receptor antagonist with anxiolytic-like properties. *Br J Pharmacol* 117:427–434.
49. Lal B, et al. (1984) Trequinsin, a potent new antihypertensive vasodilator in the series of 2-(arylimino)-3-alkyl-9,10-dimethoxy-3,4,6,7-tetrahydro-2H-pyrimido [6,1-a]isoquinolin-4-ones. *J Med Chem* 27:1470–1480.
50. Knauf U, Tschopp C, Gram H (2001) Negative regulation of protein translation by mitogen-activated protein kinase-interacting kinases 1 and 2. *Mol Cell Biol* 21:5500–5511.
51. Showalter VM, Compton DR, Martin BR, Aboud ME (1996) Evaluation of binding in a transfected cell line expressing a peripheral cannabinoid receptor (CB2): Identification of cannabinoid receptor subtype selective ligands. *J Pharmacol Exp Ther* 278:989–999.

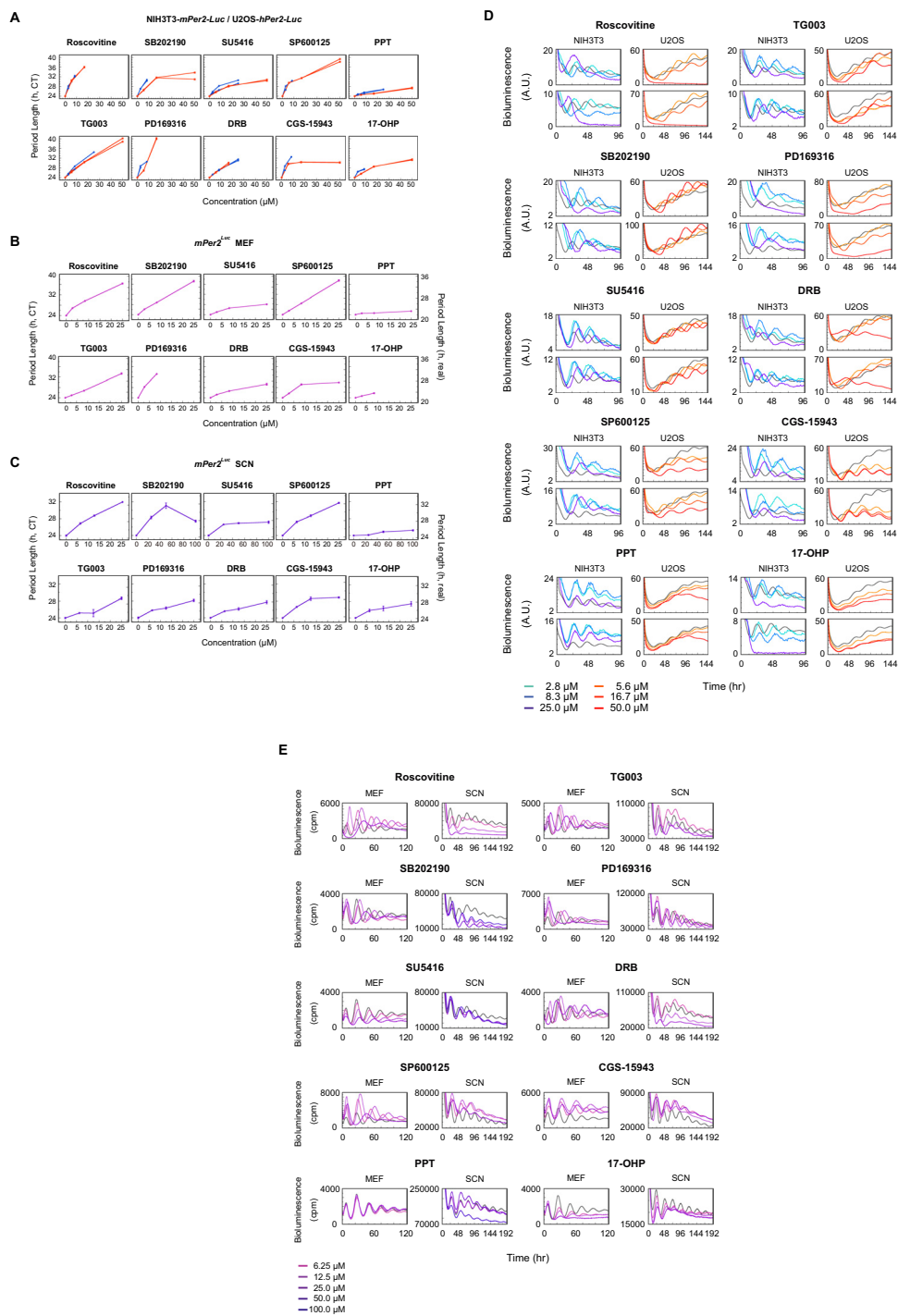


**Fig. S1.** Dose-response of period length in the NIH 3T3-*mPer2-Luc* and U2OS-*hPer2-Luc* cells (A), primary cultures of MEFs (B), slice cultures of SCN (C) from *mPer2<sup>fl/fl</sup>* mice, and raw bioluminescence data (D and E). The period length were represented both in real time (right axis in B and C) and in circadian time (i.e., the period length of control samples was adjusted to 24 h, left axis). Blue circles in (A) represented average of NIH 3T3 ( $n = 2$ ) and red squares U2OS ( $n = 3$ ). Each line represented independent experiments. Each value in (B and C) represents the mean  $\pm$  SEM. At the concentrations without data points, the cells behaved arrhythmically. (D) Time course of the reporter activity in NIH 3T3-*mPer2-Luc* cells (left panels) and U2OS-*hPer2-Luc* cells (right panels) after forskolin stimulation and the addition of compound. The gray lines represent the average of control samples ( $n = 768$  for NIH 3T3, and  $n = 96$  for U2OS) and colored lines represent the averages of samples containing compounds at the concentrations indicated at the base of the figure ( $n = 2$  for NIH 3T3, and  $n = 3$  for U2OS). The compound name is displayed at the top of each set of four panels. The upper and lower panels within each group indicate separate experiments. (E) Time course of the reporter activity in MEFs (left panels) and SCN slices (right panels) after stimulation with compound with (MEFs) or without (SCN) forskolin. The gray lines represent the average of control samples ( $n = 5$  for MEF, and  $n = 4$  for SCN) and colored lines represent the average of samples containing compound at the concentrations indicated at the bottom of the figure ( $n = 3$  for MEF, and  $n = 4$  for SCN). The compound represented in the graphs is written above each pair of panels.

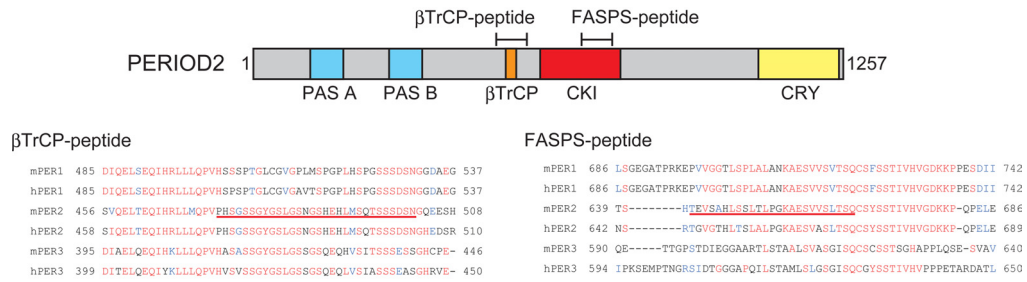




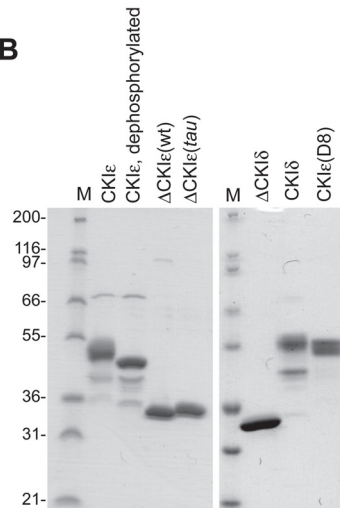




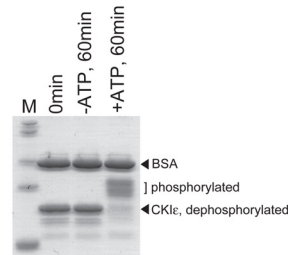
**A**



**B**



**C**



**D**

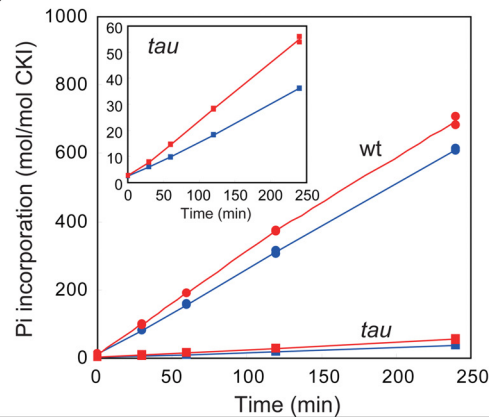


**Fig. S6.** Temperature insensitivity of the CKI<sub>ε</sub> phosphorylation activity. (A) Schematic diagram of PERIOD2 (PER2) and the sequence alignment around the  $\beta$ TrCP-binding (SSGYGS) and FASPS motif. Locations of the PAS domains (light blue), the  $\beta$ TrCP-binding motif (orange), the CKI-binding domain (red), and the CRYPTOCHROME-binding domain (yellow) are indicated. Location corresponding to the amino acid sequence of the synthetic peptide substrate is indicated by bars above the diagram. Sequence corresponding to the  $\beta$ TrCP-peptide (amino acids 473–502, a serine-rich region around the  $\beta$ TrCP-binding motif in PER2) and FASPS-peptide (amino acids 642–666, a region around FASPS-related phosphorylation sites) are underlined in the aligned sequence. (B) The catalytic domains of CKI<sub>ε</sub> (wt) and CKI<sub>ε</sub> (tau) [ $\Delta$ CKI<sub>ε</sub>(tau) and  $\Delta$ CKI<sub>ε</sub>(wt)] and full-length CKI<sub>ε</sub> were purified as described in the Materials and Methods, separated by electrophoresis, and stained with Coomassie Brilliant Blue. (C) Autophosphorylation of CKI<sub>ε</sub> before performing in vitro kinase assays. Dephosphorylated CKI<sub>ε</sub> was incubated with or without ATP for 60 min. Note that CKI<sub>ε</sub> was phosphorylated by the incubation with ATP (right-most lane). Lanes “M” in both (B) and (C) were standard molecular weight markers. (D) Phosphorylation of FASPS-peptide by  $\Delta$ CKI<sub>ε</sub>(wt) (circles) and  $\Delta$ CKI<sub>ε</sub>(tau) (squares) was assayed at 25 °C (blue) and 35 °C (red). (Inset) Expanded plot of the  $\Delta$ CKI<sub>ε</sub>(tau) phosphorylation activity. Assay conditions are described in the experimental procedures.

## Other Supporting Information Files

[Table S1](#)

[Table S2](#)

[Table S3](#)

[Table S4](#)